Dynamic Modelling of Cation Exchange Membrane Chromatography for Capturing Human Immunoglobulin G (IgG)

by

Nagma Zerin

A thesis

presented to the University of Waterloo

in fulfillment of the

thesis requirement for the degree of

Master of Applied Science

in

Chemical Engineering

Waterloo, Ontario, Canada, 2016

Author's Declaration

I hereby declare that I am the sole author of this thesis. This is a true copy of the thesis, including any required final revisions, as accepted by my examiners.

I understand that my thesis may be made electronically available to the public.

Nagma Zerin

Abstract

Membrane chromatography is an emerging technology with great potential for purification of antibodies in the biotechnology industry. To ensure the effective design and development of membrane chromatography, modelling of this system at transient state or dynamic modelling is of great importance. Until this point dynamic modelling studies have mainly focused on anion exchange and affinity membranes. In this study, dynamic modelling of membrane chromatography was performed using two commercial cation exchange membranes (Natrix C and Sartobind S) for purification of the polyclonal antibody Human IgG.

The modelling involved solving three differential equations with eight model parameters and resulted in simulated breakthrough curves for IgG. Three of the model parameters, the overall system volume (V_o), the total porosity of membrane (Ɛ) and the interstitial velocity (U) were determined experimentally using 1% acetone as tracer under two different buffer conditions at pH 5 (phosphate citrate buffer and acetate buffer). The overall range of the porosity estimates for the two membranes was 0.77-0.95, which was in agreement with published porosity values. As no research has used tracer to estimate the porosity of cation exchange membranes so far, this is one of the novel aspects of the study. Further work with an alternative method is required to confirm these porosity estimates.

To obtain experimental breakthrough curves, IgG was purified using both Natrix C and Sartobind S membranes under acetate buffer (pH 5) condition. The model breakthrough curves were fitted to the experimental breakthrough curves with MATLAB. The model fitting using Natrix C membrane was adequate as the sum of squared error (SSE) value was 0.07. However, the model fitting of the breakthrough curve for the Sartobind S membrane was inadequate due to high SSE value of 20.47. From the parameter sensitivity analysis with Natrix C, it was noted that with increasing membrane porosity, the maximum binding capacity of IgG increases.

Overall, this study generated new information regarding the porosity of cation exchange membranes and contributed in expanding research in the area of dynamic modelling of cation exchange membrane chromatography for IgG purification.

Acknowledgements

I would like to express my earnest gratitude to my supervisor Dr. Christine Moresoli for her constant support and motivation. Along with the technical knowledge, I have learnt from her how to spread knowledge with humility and treat others with patience and generosity. I am very thankful to my co-supervisor Dr. Bernard Marcos (Université de Sherbrooke, Quebec, Canada) for helping with the MATLAB code for the dynamic modelling part. His expertise in mathematical modelling is excellent and I have gained valuable knowledge from him.

I would like to thank my lab members Huayu Niu, Joseph Khouri, Rasool Nasseri, Katharina Hassel and Yung Priscilla Lai for their outstanding company and constant help during my time in the Moresoli lab. I would like to thank Jan Tobias Weggen for performing the protein binding experiments, Dr. Marc Aucoin for giving me access to the AKTA prime system in his lab and my co-op student Clara Yuan for helping me with the tracer data collection in AKTA. I express my earnest gratitude to my readers Dr. Luis Ricardez-Sandoval and Dr. Chandramouli Madhuranthakam for finding time to evaluate my thesis.

Most of all I am extremely grateful to my family members (my parents and my sisters) for their love, inspiration and consistent help in every phase of my life. Without their support I would not be able to reach where I am today.

TABLE OF CONTENTS

LIST OF FIGURES

LIST OF TABLES

NOMENCLATURE

C_o= Initial concentration of protein/Feed concentration of protein in mobile phase (mg/ml)

C_e= Equilibrium concentration of protein (mg/ml)

C= Outlet concentration of protein in mobile phase (mg/ml)

C_s= Salt counter ion concentration in mobile phase (mg/ml)

C_{in}^{CSTR}= Inlet protein concentration of CSTR (mg/ml)

C_{out}^{CSTR}= Outlet protein concentration of CSTR (mg/ml)

C_{out}^{PFR}= Outlet protein concentration of PFR (mg/ml)

c(t)= Tracer concentration measured at the outlet of the system with time

D_{ax}= Axial dispersion coefficient of protein in mobile phase (m^2/s)

F= Volumetric flow rate during protein binding (ml/min)

F'= Volumetric flow rate during tracer experimentation (ml/min)

d= Outer diameter of the interior cylinder of the membrane holder (m)

k_a= Adsorption coefficient for Langmuir model

k_d= Desorption coefficient for Langmuir model

k_{as}= Adsorption coefficient for SMA model

k_{ds}= Desorption coefficient for SMA model

K= Equilibrium constant for Langmuir model

K_s= Equilibrium constant for SMA model

L= Thickness of the interior cylinder of the membrane holder (m)

L'= Membrane stack thickness

M= Molecular weight of solute

q= Concentration of protein in membrane (mg/ml)

q_{max}= Maximum protein binding capacity (mg/ml)

q_s' = Concentration of exchangeable salt counter ions (mg/ml)

q_s= Total salt counter ion concentration on membrane (mg/ml)

Q_s= Static protein binding capacity (mg/ml)

Q_D= Dynamic protein binding capacity (mg/ml)

R_g= Radius of gyration

S= Concentration of available adsorption sites in Langmuir model

t_o= Column dead time

t_{delay}= Time delay of the system

T= Temperature

U= Interstitial Velocity of the mobile phase (m/s)

V= Volume of the membrane (ml)

V_{ads}= Volume of the adsorbent

V_c= Total volume of column

V_{int}= Interstitial volume of fluid phase

V_m= Total membrane volume (ml)

V_o= Overall system volume (ml)

V_{pore}= Volume of pores of adsorbent

V_s= Volume of the solution/binding buffer (ml)

V_{solid}= Volume of solid material of adsorbent

$V_{10\%}$= Volume of the effluent at 10% breakthrough (ml)

$V_{100\%}$= Volume of the effluent at 100% breakthrough (ml)

V_{CSTR}= Volume of CSTR (ml)

V_{PFR}= Volume of PFR (ml)

Ʊ= Protein characteristics charge

σ= Protein steric factor

v= Viscosity of solute

ʌ= Ion exchange capacity of membrane (mg/ml)

μ = Mean residence time/First moment of tracer (min)

μ_2= Second moment/variance

Ɛ = Total porosity of membrane

$Ɛ_m$ = Porosity of membrane column

ε_p = Porosity of solid phase/adsorbent

ε_r = Bed voidage of resin

ε_t = Total porosity of column

ε_v = Void fraction of column

Chapter 1: Research motivation and objective

1.1 Motivation

Antibodies are proteins produced by the B cells of the immune system in response to foreign molecules (antigens) that enter the body. Monoclonal antibodies originate from a single B cell which makes them identical, while polyclonal antibodies come from different B cells so they are not identical to each other. Due to their identical chemical structure, all monoclonal antibodies work against a specific antigen. This trait of specificity has increased the use of monoclonal antibodies (mAbs) in treatment of cancer and autoimmune diseases as well as in diagnostic tests. Herceptin is a FDA approved monoclonal antibody that is widely used in breast cancer treatment. The increase in use has led to their high demand. Significant developments have been achieved for the production of mAbs by cell culture, but limited attention has been given to their purification. Purification of monoclonal antibodies can account for up to 60% of the overall production cost (Hofer et al., 2011). It's also a relatively slow method. Thus, development of efficient purification method for monoclonal antibodies, which minimizes the cost as well as keeps pace with the regulatory standards, is a major goal for the biotechnological and pharmaceutical industries.

Monoclonal antibodies are currently produced by animal cell cultures, mostly by Chinese hamster ovary (CHO) cells. After production the monoclonal antibodies are purified by the following steps:

- Cell Harvest: Centrifugation/filtration of the cell culture to remove the cells and to obtain supernatant containing antibodies
- Antibody Capture: Capture of the antibodies from cell supernatant, typically by Protein A affinity resin chromatography
- Antibody Polishing: Removal of impurities, typically by anion exchange chromatography

In the capture step by Protein A affinity resin chromatography, the antibodies bind to the protein A ligands which are immobilized on the resin beads. This method leads to very high protein binding due to specific binding of antibodies with protein A ligands. However, there are some disadvantages. Protein A resin is quite expensive and protein A ligands can degrade during

cleaning in place (CIP) or due to enzymes present in the cell culture, leading to reduced binding efficiency (Hofer et al., 2011). Furthermore, this method requires an additional polishing step for final purification of the antibody.

Cation exchange resin chromatography is an alternative method for antibody capture as it provides comparable antibody binding capacities to affinity based resins and does not suffer from the same drawbacks. In cation exchange chromatography, resin beads have negatively charged ligands which capture positively charged antibodies. The biggest advantage of this method is the stability of the ligands against CIP and enzyme deterioration (Hofer et al., 2011). In the last couple of years a significant amount of research (Hofer et al., 2011; Wrzosek & Polakovic,2011;Wrzosek et al., 2013) has been directed to cation exchange resin chromatography for the capture of polyclonal Immunoglobulin G (IgG), which is the most abundant antibody in human serum. The reason for the widespread use of polyclonal IgG is its low cost and availability compared to mAbs. However, cation exchange membrane chromatography, where membrane sheets (made of natural/synthetic polymers) are used instead of resin beads, has not been widely explored for polyclonal IgG purification. As there are comparatively fewer studies available (Hassel & Moresoli, 2016), the feasibility of cation exchange membrane chromatography for polyclonal IgG purification requires further investigation.

In general, protein purification by membrane chromatography is considered better than resin chromatography due to lower mass transfer resistance during protein binding as well as lower operating cost and time. However, membrane chromatography has not been fully accepted for large scale manufacturing yet due to limitations such as lower protein binding capacity, non-uniform flow distribution through the membrane holder and irregular physical characteristics of the membrane, such as pore size distribution, membrane thickness and ligand density (Orr et al., 2013; Beijeren et al., 2013; Hou et al., 2015). Thus, efficient design of the membrane as well as the development of operating conditions of the system is of great importance.

Modelling of membrane chromatographic system at transient state (dynamic modelling) is highly imperative for efficient design of the membrane and the system as it can predict the specific influence of system parameters on the overall performance. Dynamic modelling involves

solving the protein mass conservation equation along with the kinetic model describing the mechanism for protein binding or adsorption on membrane. The model that takes into account the dispersion in the system can be also incorporated for improved modelling. So far, most of the dynamic modelling in membrane chromatography has been performed with anion exchange and affinity membrane systems (Yang & Etzel, 2003; Boi et al., 2007; Montesinos-Cisneros et al., 2007; Vicente et al., 2008; Vicente et al., 2011; Dimartino et al., 2011; Francis et al., 2012; Ghosh et al., 2013; Dimartino et al., 2015). Since there is limited number of studies where dynamic modelling has been performed with cation exchange membrane chromatography (Shekhawat et al., 2016), more research needs to be conducted in this area.

In general, one of the biggest challenges of dynamic modelling of chromatographic system is the experimental determination of the parameters. In literature, some of the parameters are approximated by fitting model curve to the experimental curve, and the remaining parameters are usually taken from other literature with limited explanation for their selection. The approximation procedure for one of the model parameters, the total porosity of the adsorbent (resin/membrane), is quite ambiguous. For resin chromatography, there is brief mention of using tracer method to estimate the bed voidage of resin and column porosity (Altenhoner et al., 1997; Schmidt-Traub et al., 2012; Osberghaus et al., 2012). For membrane chromatography, (Dimartino et al., 2011) estimated porosity of affinity membrane column using tracer method. However, no published research paper has reported the use of tracer method for estimating porosity of cation exchange membranes. Thus, it is important to evaluate the feasibility of the tracer method for estimating membrane porosity in detail.

1.2 Objective

The central objective of this study was to perform dynamic modelling of cation exchange membrane chromatography for capturing polyclonal Immunoglobulin G (IgG) using two types of commercial cation exchange membranes, Natrix C and Sartobind S. Three model parameters, overall system volume (V_o), total porosity of membrane (ε) and interstitial velocity (U), were determined experimentally using two types of tracer method, step input and pulse input.

The study was conducted in three parts for Natrix C and Sartobind S membranes for two different buffer systems at pH 5 (phosphate citrate buffer and acetate buffer) which are as follows:

- Determination of overall system volume from system dispersion curves obtained by step input tracer method
- Estimation of total porosity of membrane and interstitial velocity from pulse curves obtained by pulse input tracer method
- Performance of dynamic modelling to simulate breakthrough curves for IgG

Chapter 2: Basic concepts of protein purification by liquid chromatography

This chapter includes the fundamental concepts that are involved in protein purification by liquid chromatography. It describes the stages of purification, types of materials used, the methods for determining protein binding efficiency as well as literature review for cation exchange chromatography for purification of Human IgG.

2.1 Purification steps

Chromatography is the most prominent technique used to separate/purify specific components from a mixture. It involves the physical interaction of target solute in two different phases, stationary phase and mobile phase. The solute is dissolved in the mobile phase which is passed through the stationary phase.

There are two main types of chromatography:

- Liquid chromatography (solid stationary phase, liquid mobile phase)
- Gas chromatography (solid stationary phase, gaseous mobile phase)

Liquid chromatography is most commonly used in the field of biotechnology for purification of therapeutic proteins. During downstream processing, the target proteins are purified from the impurities of the cell culture by being selectively adsorbed on the surface of the solid phase, which can be either resin beads or membrane.

There are generally 5 major steps for protein purification by liquid chromatography:

- Equilibration of solid phase with mobile phase (application/binding buffer)
- Addition of protein solution (dissolved in binding buffer) and its binding with solid phase
- Washing of unbound substances/contaminants by binding buffer
- Elution of target protein from the solid phase with elution buffer
- Regeneration of solid phase by removing all substances bound to the surface (for reusable solid phase)

2.2 Buffers

2.2.1 Properties

For a liquid chromatographic system the correct choice of mobile phase is of great importance. There are some key requirements for the mobile phase which are as follows: (Schmidt-Traub et al., 2012)

- High solubility of the target component in the mobile phase
- Chemical inertness to all kinds of reactions
- Stability, purity and low viscosity
- Safety (No use of highly flammable/toxic solvent)
- Suitable pH
- Good detection properties for UV detection

In general, buffers (solutions that resist changes in pH) are used as mobile phase during protein purification as they meet all the above mentioned requirements. In acidic buffer, weak acid and its conjugate base pair are in equilibrium with each other which can be expressed as follows:

$$HA \leftrightarrow H^+ + A^- \qquad \textbf{Equation 1}$$

Weak acid Conjugate base

The Henderson-Hasselbalch equation (where [HA] is concentration of weak acid and $[A^-]$ is concentration of conjugate base) is used to estimate the pH of the buffer (Equation 2).

$$pH = pK_a + \log\left(\frac{[A^-]}{[HA]}\right) \qquad \textbf{Equation 2}$$

When 50% of the weak acid dissociates into its conjugate base, which means when $[A^-] = [HA]$, $pH = pK_a$.

2.2.2 Common buffers for protein purification

Three buffers that are quite commonly used for protein purification are acetate buffer, phosphate citrate buffer and phosphate buffer due to their stability and safety.

In acetate buffer acetic acid (CH_3COOH) dissociates in one step (Mohan, 2003):

$$CH_3COOH \leftrightarrow CH_3COO^- + H^+ \quad (pK_a=4.75) \qquad \textbf{Equation 3}$$

In phosphate citrate buffer the citric acid ($C_6H_8O_7$) dissociates in 3 steps (Nozawa et al., n.d.):

$$C_6H_8O_7 \leftrightarrow C_6H_7O_7^- + H^+ \quad (pK_a=3.13) \qquad \textbf{Equation 4}$$

$$C_6H_7O_7^- \leftrightarrow C_6H_6O_7^{2-} + H^+ \quad (pK_a=4.76) \qquad \textbf{Equation 5}$$

$$C_6H_6O_7^{2-} \leftrightarrow C_6H_5O_7^{3-} + H^+ \quad (pK_a=6.4) \qquad \textbf{Equation 6}$$

For phosphate buffer the dissociation of the phosphoric acid (H_3PO_4) also occurs in 3 steps (Phosphate Buffers, n.d.):

$$H_3PO_4 \leftrightarrow H_2PO_4^- + H^+ \quad (pK_a=2.12) \qquad \textbf{Equation 7}$$

$$H_2PO_4^- \leftrightarrow HPO_4^{2-} + H^+ \quad (pK_a=7.21) \qquad \textbf{Equation 8}$$

$$HPO_4^{2-} \leftrightarrow PO_4^{3-} + H^+ \quad (pK_a=12.44) \qquad \textbf{Equation 9}$$

2.3 Resin and membrane Chromatography

2.3.1 Configuration of resin and membrane chromatography

Column chromatography is the most common configuration for liquid chromatography where porous/nonporous resin beads are packed inside a column which is usually made of glass, polymer or stainless steel, and the mobile phase (binding buffer containing protein) flows through the beads. For membrane chromatography, microporous/macroporous membrane, made from natural or synthetic polymers, is placed inside a membrane holder.

Typically three types of membrane adsorbers are used: flat sheet, hollow fibre and radial flow. Flat sheet membranes are the most widely used geometry for membrane chromatography, where liquid is introduced perpendicularly to the membrane surface. Stacks of flat sheet membranes is a preferred way due to increased binding efficiency (Ghosh, 2002; Saxena et al., 2009). A hollow fiber membrane has a tubular shape, where liquid initially flows parallel to the membrane surface and then gets directed towards the pores. The radial flow membranes are prepared by wrapping a flat sheet membrane over a porous cylindrical core spirally (Ghosh, 2002; Saxena et al., 2009). The overall liquid flow through the radial flow membrane is mostly in a normal direction.

2.3.2 Material of solid phase

The solid phase (resin/membrane) has a base material which is usually modified with specific ligands. The base materials for resins can be either made from inorganic materials (e.g., silica, porous glass) or cross-linked organic polymers (e.g., polysaccharides, polyacrylates, synthetic copolymers, polymer composites) (Muller, 2005). The base materials for membranes are always made from polymers. The materials that are most frequently used for membranes are regenerated cellulose, polyethersulfone and polyvinylidene fluoride which get modified by chemical activation, coating or grafting (Boi, 2007). The proper surface modification of the base material is very crucial since it affects protein binding capacity, mass transfer property and non-specific interaction of the solid phase with the protein, which ultimately impacts the adsorption efficiency.

For membrane chromatography, the membranes can also be classified based on the functionalization of the interior pore surface:

- Membranes with pore surface grafted with functionalized polymer layer
- Membranes with pore surface containing functionalized hydrogel layer

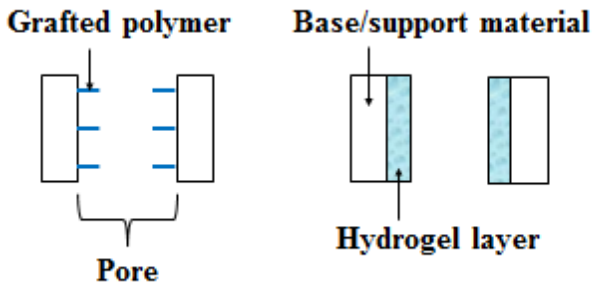

Figure 1: Types of membrane based on interior pore surface functionalization

Hydrogel is made of crosslinked hydrophilic polymer chains that can contain large amount of water, resulting in a gel like structure. Inside the pores of the gel layer the functional groups are attached. It is generally accepted that hydrogel membranes have comparatively higher protein binding capacity because of the increased functional group density of the gel layer.

It is important to note that pore size is a crucial criterion for the overall performance of membrane chromatography. The pore size should be large enough for sufficient access of large proteins to the functional groups inside the pores.

2.3.3 Performance of resin and membrane chromatography

There are significant differences between resin and membrane chromatography in terms of their operating conditions and performance which are listed in Table 1.

Table 1: Comparison between resin and membrane chromatography for protein purification applications (Charcosset, 1998; Ghosh, 2002; Yang et al., 2011; Ghosh et al., 2013; Orr et al., 2013; Beijeren et al., 2013)

Parameter	Resin Chromatography	Membrane Chromatography
Pressure drop	High	Low (due to large pore size, typically in between 0.1-20 μm)
Dominant transport	Diffusion	Convection
Mass transfer resistance	Higher	Lower
Processing time	Long	Relatively Short
Scaling up	Harder	Easier
Protein binding capacity	Higher	Lower
Use of high flow rate	No	Yes
Cost of solid phase	High	Low
Disposal of solid phase	No (Resins are regenerated)	Yes

Generally membrane chromatography has better properties than resin chromatography. One of the key properties that makes membrane chromatography more preferable than resin chromatography is its lower mass transfer resistance. The ligands or functional groups on the surface of the membrane pores are along the path of the feed flow through the membrane (Figure 2). Thus, the target proteins can access the binding sites directly by bulk convection, which significantly reduces mass transport limitations. In resin chromatography, however, proteins have to diffuse through the pores in the resin beads to reach binding sites (Figure 2). This increases the process time during protein elution for resin chromatography since transport by diffusion is quite slow. In addition, membrane chromatography doesn't require column packing and is very useful for separation of large protein molecules with weight-average molecular

weight greater than 150 kDa (Tatarova et al., 2009). However, due to lower protein binding capacity, membrane chromatography has not been widely adopted and would hugely benefit from process development.

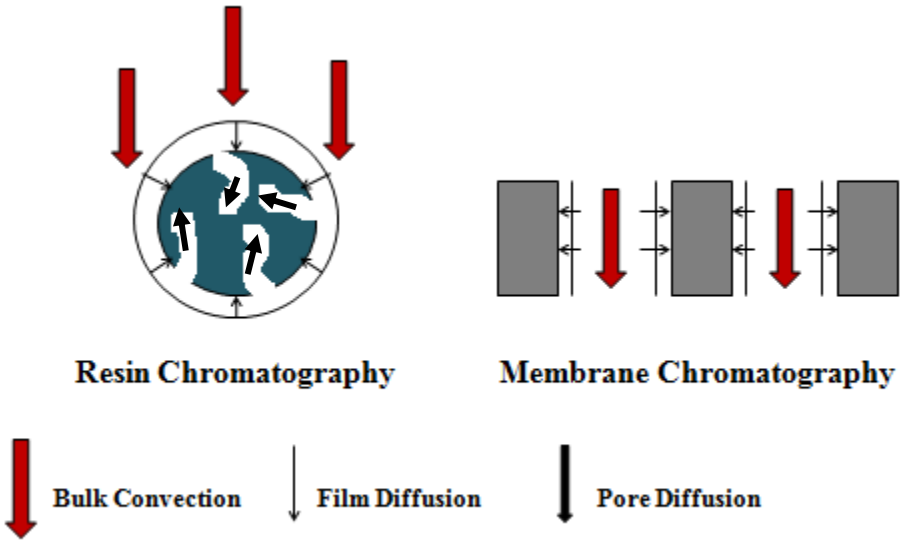

Figure 2: Mass transport comparison in resin chromatography and membrane chromatography (Adapted from Orr et al., 2013)

2.4 Principles of ion exchange chromatography

In ion exchange chromatography, operating conditions are selected such that charged proteins adsorb on oppositely charged solid phase (resin/membrane) due to electrostatic attraction. The charge of the adsorbent is based on the ligands/functional groups immobilized on its surface. For instance in cation exchange chromatography, the adsorbent has negatively charged ligands and the adsorbed proteins have net positive charge (Figure 3). In contrast for anion exchange chromatography, the adsorbent has positively charged ligands and the adsorbed proteins have net negative charge.

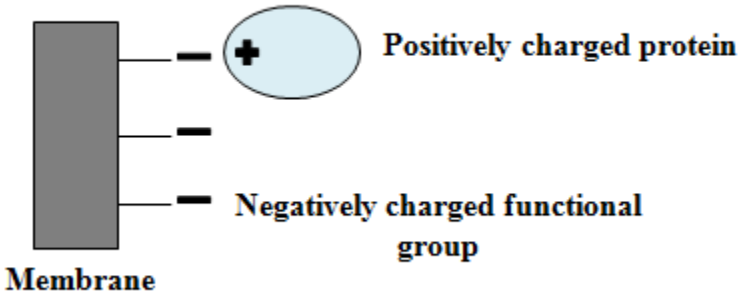

Figure 3: Diagram of cation exchange membrane chromatography

Strong ion exchangers stay ionized within a wide range of pH, while weak ion exchangers stay ionized within a limited range of pH. For instance, cation exchangers which have sulphonic functional group ($-SO_3^-$) or sulphopropyl functional group ($-CH_2-CH_2-CH_2-SO_3^-$) are strong, while those which have carboxyl group ($-COO^-$) are weak. The anion exchangers which have quaternary amine groups ($N(CH_3)_4^+$) are strong, while those which have primary amine groups (NH_3+) are weak.

In ion exchange chromatography, the net charge of the protein is the most important factor. Every protein has a particular pH where the positively and negatively charged amino acid residues are balanced and the net charge of the protein is zero. This pH is known as the isoelectric point (pI). Above pI the net charge of the protein is negative, while below pI the net charge of the protein is positive. Thus, the pH of the binding buffer is a very significant

operating condition. In cation exchange chromatography the pH of the binding buffer is usually chosen in a way so that it is greater than the pK_a of the negatively charged groups on the solid phase and smaller than the isoelectric point (pI) of the protein to ensure that the protein surface mostly has positive charge.

In terms of ionic strength, the binding buffer should have low ionic strength so that the competition between the ions of the buffer and the charged proteins to be adsorbed on the solid phase is relatively small and the proteins can bind to the solid surface easily. In contrast, the elution buffer should have high ionic strength so that the competition between the ions of the buffer and the charged proteins is very high. The high amount of ions present in the elution buffer will replace the charged proteins from the surface of the solid phase resulting in protein elution.

Table 2 provides some examples of commercially available ion exchange chromatography resins and membranes.

Table 2: Examples of commercially available chromatographic ion exchange resins and membranes

Chromatography Type	Type of adsorbent	Commercial name of adsorbent	Adsorbent Material	Functional Group	Manufacturer	Pore size	Target proteins
Cation exchange	Flat sheet membrane (Sartobind S A4 Sheet, n.d.)	Sartobind S	Stabilised reinforced cellulose	Sulphonic Acid	Sartorius	3-5 µm	Monoclonal antibody (IgG), Lysozyme, BSA
	Resin (Fractogel EMD SO_3 (M), n.d.)	Fractogel EMD SO_3^- (M)	Polymethacryl -ate/ tentacle	SO_3-	Merck Millipore	100 nm	Lysozyme, Chymotrypsino-gen A, Cytochrome C
Anion exchange	Flat sheet Membrane (Sartobind Q Single Step, n.d.)	Sartobind Q	Stabilised reinforced cellulose	Quaternary Ammonium	Sartorius	3-5 µm	BSA, IgM, Plasma proteins, Lysozyme
	Resin (Fractogel EMD TMAE (M), n.d.)	Fractogel EMD TMAE (M)	Methacrylate/ tentacle	Trimethylam -inoethyl	Merck Millipore	100 nm	Conalbumin, HSA

2.5 Protein binding capacity

The overall performance of the membrane chromatographic process for protein purification (efficiency of protein binding) is evaluated by two methods: static binding capacity and dynamic binding capacity.

2.5.1 Static binding capacity

Static binding experiments are performed in a batch mode where the protein solution and membrane are mixed for binding. In this mode the proteins in the liquid phase and those bound in membrane remain in equilibrium.

The static protein binding capacity is defined as the amount of protein adsorbed per volume (or mass) of membrane which can be expressed by Equation 10.

$$Q_S = (C_o - C_e)\frac{Vs}{V} \qquad \textbf{Equation 10}$$

Here,

Q_S= Static protein binding capacity (mg/ml)

C_o= Initial concentration of protein (mg/ml)

C_e= Equilibrium concentration of protein (mg/ml)

V= Volume of the membrane (ml)

V_s= Volume of solution/ binding buffer (ml)

The static protein binding capacity for different equilibrium protein concentrations are used to create adsorption isotherm (Figure 4). The adsorption isotherms can be explained by different models which will be discussed in Chapter 3.

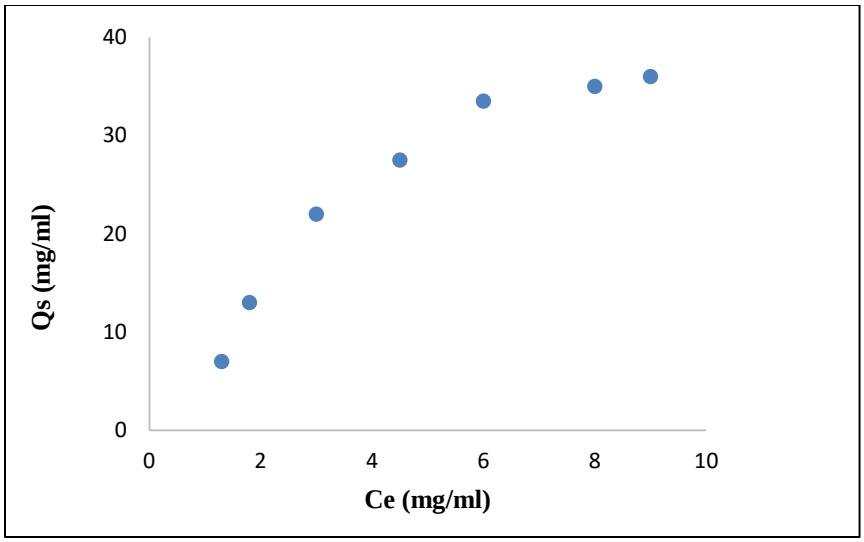

Figure 4: Example of adsorption isotherm

2.5.2 Dynamic binding capacity

Dynamic protein binding experiments are performed in a continuous mode where the protein solution is continuously fed to the membrane until breakthrough occurs, which is an indication that the membrane has been completely saturated with protein. Once membrane saturation is reached, the outlet protein concentration will be similar to the inlet protein concentration.

A breakthrough curve is a plot of C/C_o (outlet protein concentration/feed protein concentration) versus time or volume of the effluent (Figure 5). When C/C_o reaches 1, it means that the membrane has been completely saturated with protein. The area above the breakthrough curve represents the amount of protein retained in membrane, while that below represents the amount of protein that is not retained in membrane and therefore is lost with the effluent solution.

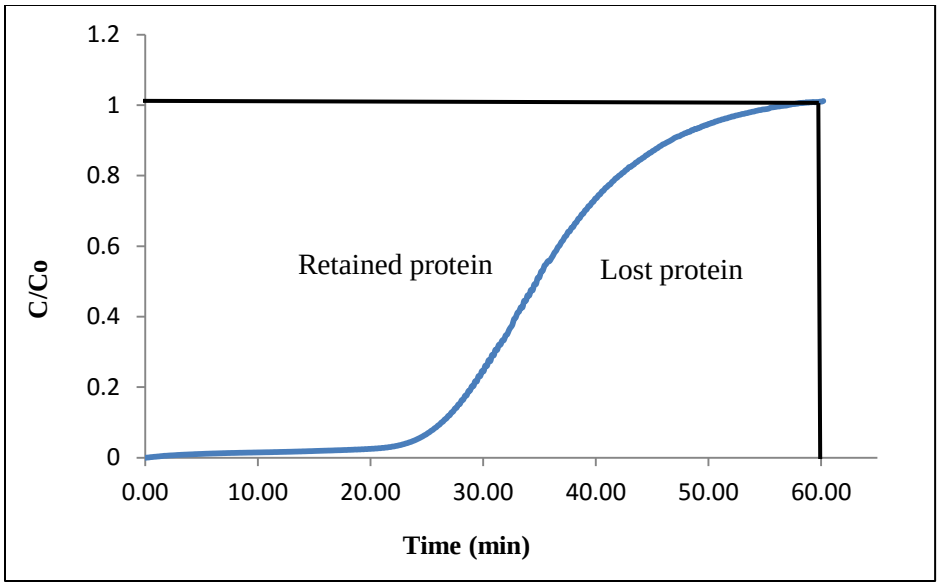

Figure 5: Example of breakthrough curve using time of effluent

For membrane chromatography the dynamic protein binding capacity is typically defined as the amount of protein adsorbed per volume (or mass/area) of membrane at 10% breakthrough (concentration of the outlet protein is 10% of the feed protein concentration) or 100% breakthrough (concentration of the outlet protein is equal to the feed protein concentration) which can be expressed by Equations 11 and 12 respectively (Wrzosek et al., 2013).

$$Q_{D(10\%)} = \frac{\int_{Vo}^{V10\%}(C_o - C)dv}{V} \qquad \textbf{Equation 11}$$

$$Q_{D(100\%)} = \frac{\int_{Vo}^{V100\%}(C_o - C)dv}{V} \qquad \textbf{Equation 12}$$

Here,

Q_D= Dynamic protein binding capacity (mg/ml)

C_o= Feed concentration of protein in mobile phase (mg/ml)

C= Outlet concentration of protein in mobile phase (mg/ml)

V= Volume of the membrane (ml)

$V_{10\%}$= Volume of the effluent at 10% breakthrough (ml)

$V_{100\%}$= Volume of the effluent at 100% breakthrough (ml)

V_o= Overall system volume (ml)

2.6 Immunoglobulin G (IgG) characteristics and purification

Type G immunoglobulin (IgG) is the most abundant antibody of all in the human serum immunoglobulins and it is a Y shaped glycoprotein (containing protein and carbohydrate component). It is comprised of two heavy chains and two light chains which are linked together by inter-chain disulfide bonds. The two heavy chains and the two light chains are identical. There are two fragments for antibody binding (F_{ab}) consisting of one segment of the heavy chain and one segment of the light chain, and one crystallisable fragment (F_c) consisting of heavy chain segments (Figure 6). The variable domains of F_{ab} regions are the most important regions in antibody which bind in a lock and key mechanism with their specific antigens. Both F_{ab} and F_c regions also have constant domains.

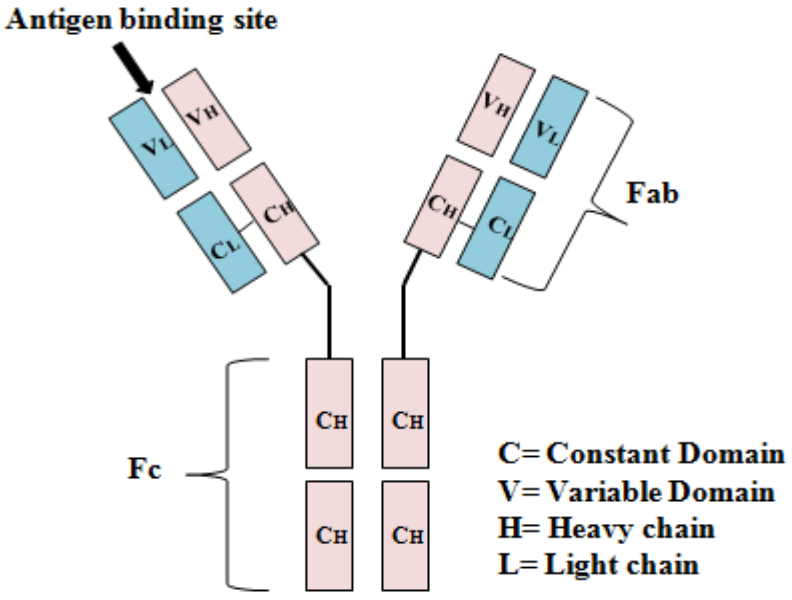

Figure 6: Structure of IgG

Polyclonal IgG molecules are produced by different B cells of the immune system, while monoclonal IgG come from the same B cells. In a mixture of polyclonal IgG molecules, each of them binds to a specific antigen. These molecules can be produced by injecting a mammal (e.g. mouse, rabbit) with an antigen which stimulates the B cells. The produced polyclonal IgG can be later isolated from the blood serum of the mammal.

Polyclonal IgG has a molecular weight of approximately 150 kDa (Antibody Basics, n.d.) and isoelectric point in the pH range of 6.5-10, where 77% molecules have pI between pH 8-10 (Wrzosek & Polakovic, 2011). Thus, during cation exchange chromatography the pH of the binding buffer is selected usually around 5 so that the net charge of IgG is positive. The positively charged IgG molecules interact with the negative functional groups or ligands of the cation exchange membranes.

Table 3 lists the static and dynamic binding capacities of IgG for cation exchange chromatography along with the information on adsorbents and operating conditions from some recent literature.

Table 3: Binding capacities of Human IgG using cation exchange chromatography

Type of Adsorbent	Cation exchanger	Particle and pore size	Static Binding		Dynamic Binding	
			Maximum Capacity	Buffer	Maximum Capacity	Buffer
Membrane	Natrix C (Hassel & Moresoli, 2016)	Pore size >0.3 µm	20.1±1.5 mg/ml (pH 4.8)	Binding and Elution buffer: Phosphate Citrate buffer	109.1±1.8 mg/ml (pH 5)	Binding and Elution buffer: 50 mM Acetate buffer
Resin	Fractogel® EMD SO_3 (M), Fractogel® EMD COO (M), Capto ™ MMC (Hofer et al., 2011)	Fractogels: Particle size (40-90 µm) Pore size: 800 A° Capto ™ MMC: Particle size (70 µm)	For 0 mM NaCl: Fractogel® EMD SO_3 (M): 120 mg/ml (pH 5) Fractogel® EMD COO (M): Almost 50 mg/ml (pH 5.5) Capto ™ MMC: Almost 70 mg/ml (pH 5.5)	Binding buffer: 25 mM acetate/phosphate buffer +0-300 mM NaCl (pH 4.5- 7.5) Elution buffer: 25 mM acetate/phosphate buffer +1 M NaCl (pH same as binding buffer)	-	-
Resin	Polymethyl methacrylate matix+ sulfoisobutyl ligand (Wrzosek & Polakovi˘c, 2011)	Mean pore radius (27 nm-34 nm), Porosity (0.79-0.81)	Almost 155 mg/ml for pH 5 and ligand density 509 µmol/g	Binding buffer: 50 mM sodium citrate phosphate buffer (pH 4-7)+ 0 mM or 75 mM NaCl	-	-
Resin	Fractogel EMD SE Hicap (M) (Wrzosek et al., 2013)	Mean particle diameter (65 µm), Particle porosity (0.7)	166±8 mg/g for 0 mM NaCl in binding buffer	Binding buffer: 50 mM Phosphate citrate buffer (pH 4.5) + (0 mM/75 mM/ 150 mM NaCl)	127 mg/g for 0mM NaCl in binding buffer and 0.2 ml/min flow rate	Binding buffer: 50 mM Phosphate citrate buffer (pH 4.5) + (0 mM/75 mM/ 150 mM NaCl) Elution buffer: 50 mM Phosphate citrate buffer (pH 4.5) + 1M NaCl

Chapter 3: Ion exchange membrane chromatographic modelling

Mathematical modelling is important for proper design, selection, operation and analysis of liquid chromatographic system. It can be used to predict the influence of system parameters on protein binding performance. This chapter reviews the concepts of dynamic modelling for ion exchange membrane chromatographic system to capture proteins at transient condition.

The modelling is based on the protein mass conservation equation along with the kinetic equation describing protein adsorption on membrane and the differential equation describing dispersion in the chromatographic system.

3.1 Assumptions and transport mechanisms

There are some assumptions for the dynamic modelling of liquid chromatographic system which are applicable for ion exchange membrane chromatographic system as well. They are as follows: (Schmidt-Traub et al., 2012)

- The density and viscosity of the mobile phase are constant.
- Radial distributions are negligible.
- Axial dispersion coefficient is constant.
- The process is isothermal.

There are three types of transport mechanisms during protein capture by membrane:

- Mass transport of proteins in the bulk solution through convection and axial dispersion
- Diffusion of proteins through liquid film layer and grafted polymer layer or hydrogel layer inside the membrane pore surface
- Adsorption of proteins to the functional groups inside membrane pores and their desorption

The diffusion of protein through liquid film layer as well as grafted polymer or hydrogel layer is often neglected for membrane chromatographic system as convection, axial dispersion and adsorption or desorption of proteins are considered as the major transport phenomena (Dimartino et al., 2011). For ion exchange chromatography it is considered that the adsorption kinetics of protein is very fast. Therefore, the mass transport of protein becomes the rate limiting step (Beijeren et al., 2013).

3.2 Protein mass conservation

The protein mass balance for a membrane chromatographic system is performed on the membrane holder containing one or multiple membranes. The mass conservation equation is written as follows:

$$\frac{\partial C}{\partial t} + \frac{1-\varepsilon}{\varepsilon}\frac{\partial q}{\partial t} + U\frac{\partial C}{\partial x} = D_{ax}\frac{\partial^2 C}{\partial x^2} \qquad \textbf{Equation 13}$$

Here,

C= Outlet concentration of protein in mobile phase (mol/m^3)

q= Concentration of protein in membrane (mol/m^3)

Ɛ= Total porosity of membrane

U= Interstitial velocity of the mobile phase (m/s)

D_{ax}= Axial dispersion coefficient of protein in mobile phase (m^2/s)

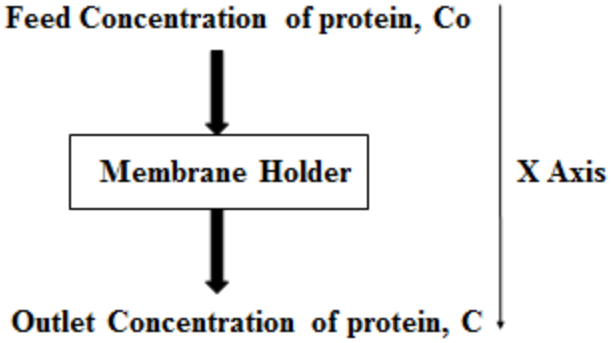

Figure 7: Schematic representation of the protein mass conservation in membrane chromatographic system

The mass conservation equation is also known as the transport dispersive model assuming a dispersed flow through the membrane (Beijeren et al., 2012). The unknown parameters from Equation 13 are Ɛ, U and D_{ax}.

Initial and Boundary conditions:

a) Initial condition: At t=0

$$C(x,0)=0 \qquad \textbf{Equation 14}$$

$$q(x,0)=0 \qquad \textbf{Equation 15}$$

b) Dankwert's Boundary conditions: (Beijeren et al., 2012)

1. At the entrance of the membrane (x=0):

$$U\,[C_o - C(x=0, t)] = -D_{ax}\frac{\partial C}{\partial x}(x=0, t) \qquad \textbf{Equation 16}$$

Here,

C_o= Feed concentration of protein in mobile phase

C(x=0, t) = Protein concentration at position x=0 for time t

$\frac{\partial C}{\partial x}$ (x=0, t) = Gradient of protein concentration at position x=0 for time t

2. At the exit of the membrane (x=L):

$\frac{\partial C}{\partial x}$ (x=L, t)=0 **Equation 17**

Here,

$\frac{\partial C}{\partial x}$ (x=L, t)= Gradient of protein concentration at position x=L for time t

In a system where the flow is continuous, some molecules in the fluid can diffuse forward ahead of the molar average velocity of the fluid flow, while the others can lag behind. This process is known as convective diffusion or dispersion. When dispersion is considered in the axial direction it is called axial dispersion. In a chromatographic system broadening of the signal of the protein concentration occurs due to dispersion, which is represented by the axial dispersion coefficient term in the mass conservation equation (Equation 13).

3.3 Kinetics of protein adsorption

There are different kinetic models that explain the protein adsorption on a solid phase in liquid chromatographic systems. The two most prominent ones for ion exchange chromatography are the Langmuir Model and the Steric Mass Action Model.

3.3.1 Langmuir model for protein adsorption

It is one of the most commonly used model due to its simplicity. The model assumes that all adsorption sites on the adsorbent (membrane) are identical, each adsorption site is independent where one protein molecule adsorbs on one site and doesn't have any effect on another molecule adsorbed on a nearby adsorption site (Figure 8).

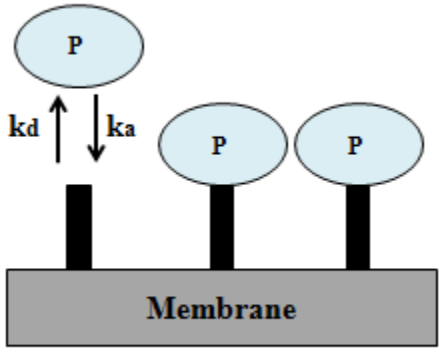

Figure 8: Schematic representation of protein (P) binding on adsorption sites according to Langmuir model

Considering a membrane with a fixed number of adsorption sites on which protein molecules (P) bind reversibly in a monolayer pattern, the adsorption of protein can be written as follows:

$$C + S \underset{k_d}{\overset{k_a}{\leftrightarrow}} q \qquad \textbf{Equation 18}$$

Here C and q represent the protein concentration in mobile phase and in membrane respectively. The constants k_a and k_d are the adsorption and desorption coefficients respectively.

The concentration of available adsorption sites, represented by S is the difference between the maximum number of adsorption sites and the number of occupied adsorption sites.

The rate of protein binding for the Langmuir model is given as:

$$\frac{\partial q}{\partial t} = k_a C (q_{max} - q) - k_d q \qquad \textbf{Equation 19}$$

When rapid equilibrium is assumed, $\frac{\partial q}{\partial t}$ can be considered to be almost zero. In that case Equation 19 can be written as:

$$k_a C (q_{max} - q) - k_d q = 0 \qquad \textbf{Equation 20}$$

$$K = \frac{q}{C(q_{max} - q)} \qquad \textbf{Equation 21}$$

Here K is the equilibrium constant which is the ratio of k_a and k_d and q_{max} is the maximum protein binding capacity. Rearranging Equation 21 leads to the Langmuir model for static binding.

$$q = q_{max} \frac{KC}{1+KC} \qquad \textbf{Equation 22}$$

Langmuir model has three model parameters for dynamic condition (q_{max}, k_a and k_d) which makes it easy to use. Thus, in this study Langmuir model has been used to describe protein adsorption on membrane. However, it should be noted that the model has some constraints. It gives a good representation of the adsorption for proteins only when the protein has small size and the protein adsorbed on one site doesn't have any effect on another protein adsorbed on a nearby adsorption site. The model also doesn't take into account the effect of ionic strength of buffer, an important consideration for protein adsorption by ion exchange membrane, and does not account for the multi-pointed nature of protein binding (Chen et al., 2006).

3.3.2 Steric Mass Action (SMA) model for protein adsorption

To address limitations of the Langmuir model, more sophisticated models have been developed with time. For example, the Steric Mass Action (SMA) model was proposed by (Brooks & Crammer, 1992) to describe non-linear adsorption in ion exchange chromatography. The SMA model assumes the following (Brooks & Crammer, 1992):

- The solution and the adsorbed phases are thermodynamically ideal.
- Multi-pointed nature of protein can be represented by experimentally determined protein characteristic charge.
- The binding of large proteins causes steric hindrance of the salt counter ions bound on the adsorbent. This makes the salt counter ions unavailable for exchange with other free proteins in the solution.
- Effect of co-ions and factors that can influence the tertiary structure or protein is negligible.
- The model parameters are constant and independent of protein and salt counter ion concentration.

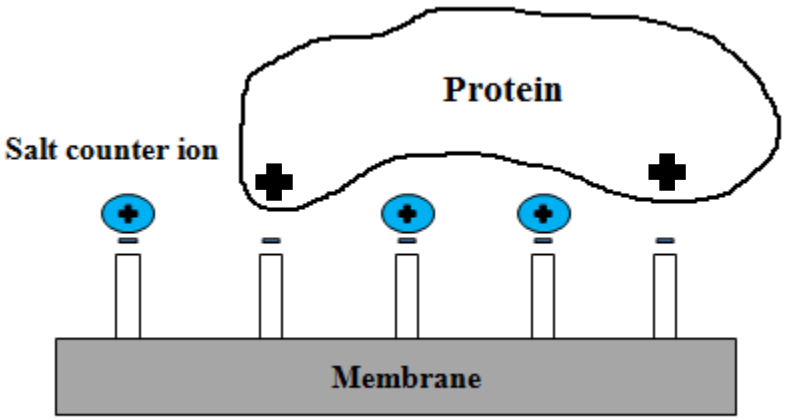

Figure 9: Schematic representation of protein binding on adsorption sites and steric hindrance of salt counter ions according to SMA model (Adapted from Brooks & Crammer, 1992)

For ion exchange membrane chromatography, the stoichiometric exchange of protein and exchangeable salt counter ions is expressed as follows:

$$C + \upsilon\, q_s' \underset{k_{ds}}{\overset{k_{as}}{\longleftrightarrow}} q + \upsilon\, C_s \qquad \textbf{Equation 23}$$

Here,

C= Concentration of protein in mobile phase (mg/ml)

C_s= Salt counter ion concentration in mobile phase (mg/ml)

q= Concentration of protein in membrane (mg/ml)

q_s'= Concentration of exchangeable salt counter ions (mg/ml)

k_{as}= Adsorption coefficient for SMA model

k_{ds}= Desorption coefficient for SMA model

υ= Protein characteristic charge

The kinetic equation for protein binding can be written as follows:

$$\frac{\partial q}{\partial t} = k_{as}\, C q_s'^{\upsilon} - k_{ds}\, C_s^{\upsilon}\, q \qquad \textbf{Equation 24}$$

When rapid equilibrium is assumed, $\frac{\partial q}{\partial t}$ can be considered to be nearly zero. In that case equation 24 is reduced to the following equation:

$$k_{as} C q_s'^{\upsilon} - k_{ds}\, C_s^{\upsilon}\, q = 0 \qquad \textbf{Equation 25}$$

$$K_s = \frac{q\, Cs^{\upsilon}}{C\, q_s'^{\upsilon}} \qquad \textbf{Equation 26}$$

Here K_s is the equilibrium constant which is the ratio of k_{as} and k_{ds}.

The ion exchange capacity of membrane (ʌ) and total salt counter ion concentration on membrane (q_s) can be represented by the following equations:

$$ʌ = q_s + Ʊq \qquad \textbf{Equation 27}$$

$$q_s = q_s' + \sigma q \qquad \textbf{Equation 28}$$

Here σ is protein steric factor.

By combining Equation 27 and 28:

$$q_s' = ʌ - (Ʊ+\sigma)\, q \qquad \textbf{Equation 29}$$

After substituting q_s' in Equation 26 and rearranging, the protein binding capacity according to the SMA model for static binding can be written as:

$$q = K_s C \left[\frac{ʌ-(Ʊ+\sigma)q}{C_s}\right]^{Ʊ} \qquad \textbf{Equation 30}$$

3.4 System Dispersion

3.4.1 Conventional dispersion model

The experimental system in membrane chromatographic method consists of membrane holder containing one membrane/membrane stack as well as external elements like pump, valves, connecting tubing, detector cell etc. While passing through all these elements the flow of the protein solution deviates from pure plug flow and results in a dispersed flow.

A conventional method to describe protein dispersion in membrane chromatographic system is the use of combination of Continuous Stirred Tank Reactor (CSTR) and Plug Flow Reactor (PFR). In published modeling studies, the combined CSTR-PFR series has been placed before (Boi et al., 2007; Dimartino et al., 2011) or after the membrane stack (Yang et al., 1999; Boi, 2007) (Figure 10). The CSTR takes into account the mixing effects, while the PFR represents the time delay and dead/stagnant volume effects.

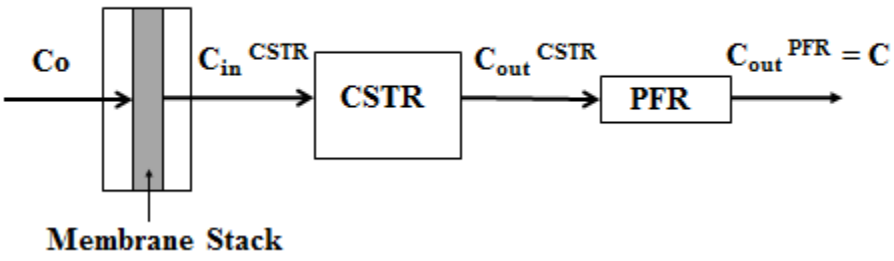

Figure 10: Conventional dispersion model for membrane chromatography

The overall system volume representing mixing and time delay effects can be expressed as the summation of the volumes of the two hypothetical reactors:

$$V_o = V_{CSTR} + V_{PFR} \qquad \textbf{Equation 31}$$

Here, V_{CSTR} is the volume of CSTR and V_{PFR} is the volume of PFR.

The protein mass balance for the CSTR is expressed as follows:

$$\frac{dC_{out}^{CSTR}}{dt} = \frac{F}{V_{CSTR}}(C_{in}^{CSTR} - C_{out}^{CSTR}) \qquad \textbf{Equation 32}$$

Here, C_{in}^{CSTR} and C_{out}^{CSTR} represent the inlet and outlet protein concentrations of CSTR, F is the volumetric flow rate during protein binding and V_{CSTR} is the volume of the CSTR.

Using Equation 31 V_{CSTR} in Equation 32 can be written as V_o - V_{PFR} where V_o and V_{PFR} both are unknown parameters.

Initial condition: At t=0, $C_{out}^{CSTR} = 0$ **Equation 33**

When the PFR is located after the CSTR, the outlet protein concentration of PFR can be represented by Equation 34, where t_{delay} is the time delay of the system (V_{PFR}/F) and C is the outlet concentration of protein in mobile phase.

$$C_{out}^{PFR} = \begin{cases} 0 & t<t_{delay} \\ C & t >= t_{delay} \end{cases} \qquad \textbf{Equation 34}$$

3.4.2 Zonal Rate Model (ZRM) for membrane holder only

(Francis et al., 2012) and (Ghosh et al., 2013) focused on protein dispersion inside the membrane holder only specifically and developed Zonal Rate Model (ZRM). ZRM divided the hold-up volumes before and after the membrane stack as well as in the membrane stack into different zones. The model accounted for differences in the path lengths of protein while entering or leaving the membrane stack (Figure 11). The hold-up volumes before and after the membrane stack were represented by a network of virtual CSTRs and each of the CSTR was modelled by Equation 32.

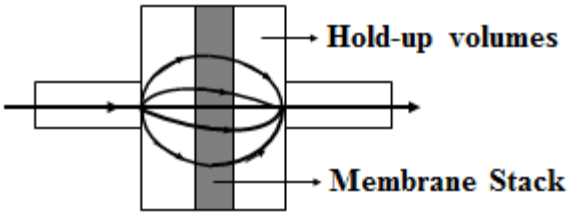

Figure 11: Schematic for Zonal Rate Model considering protein dispersion in membrane holder only (adapted from Ghosh et al., 2013)

The PFR describing time delay was decoupled from the system and placed in the network of CSTRs arbitrarily.

3.5 Parameters for dynamic modelling of protein capture

3.5.1 Parameters

To perform dynamic modelling for protein capture in a membrane chromatographic system, the protein mass conservation equation (Equation 13), Langmuir model (Equation 19) and conventional dispersion model (Equation 32) are solved simultaneously. The known parameters include the feed concentration of protein in the mobile phase (C_o) and the volumetric flow rate during protein binding (F).

There remains 8 unknown parameters to be estimated:

- Overall system volume (V_o)
- Total porosity of membrane (ε)
- Interstitial velocity of the mobile phase (U)
- Volume of PFR (V_{PFR})
- Axial dispersion coefficient (D_{ax})
- Adsorption coefficient (k_a)
- Desorption coefficient (k_d)
- Maximum protein binding capacity (q_{max})

V_o, ε and U can be determined from tracer experiments. V_{PFR} and D_{ax} can be estimated from literature. The parameters of Langmuir model k_a, k_d and q_{max} can be estimated by minimizing the sum of squared error (SSE) during model fitting of the experimental protein breakthrough curve.

3.5.2 Tracer Experimentation

Information on the overall system volume and flow non-idealities of membrane chromatographic system can be obtained from dispersion curves of a non-binding and non-interacting substance known as tracer, which is fed to the system and monitored at the outlet of the system. An ideal tracer should be easily detectable, completely soluble in mobile phase, should not be retained by adsorbent and should have similar molecular size as the component to be separated (Schmidt-Traub et al., 2012). Typical substances used as tracer are acetone and

dextran (Altenhoner et al., 1997; Osberghaus et al., 2012; Dimartino et al., 2011; Teepakorn et al., 2015). In this study, acetone was chosen as the tracer due to its low cost.

There are two experimental tracer methods (Fogler, 2006):

- Pulse input tracer method: Injection of a known amount of tracer for a very short time interval in the feed stream entering the system.
- Step input tracer method: Addition of a known amount of tracer at constant flow rate at the entrance of the system.

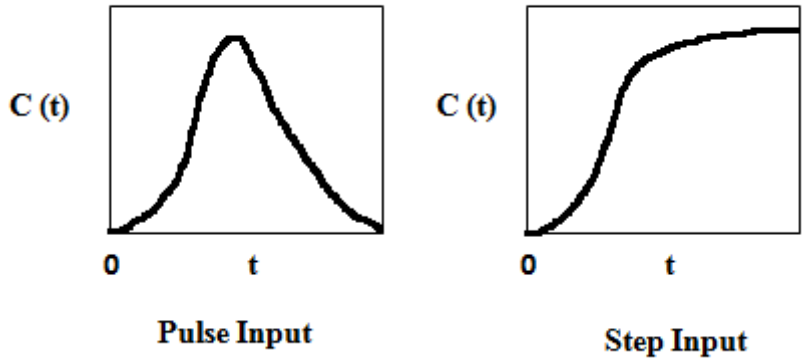

Figure 11 : Response of two kinds of tracer experiments, Pulse input (left) and Step input (right)

When the pulse input tracer method is used, the first moment of the tracer can be calculated from the tracer concentration at the outlet of the system.

First moment or Mean residence time of tracer (Dimartino et al., 2011):

$$\mu = \frac{\int_0^\infty t\, c(t)dt}{\int_0^\infty c(t)dt} \qquad \textbf{Equation 35}$$

Here c (t) is the tracer concentration measured at the outlet of the system with time

Second moment or Variance (Dimartino et al., 2011):

$$\mu_2 = \frac{\int_0^\infty (t-\mu)^2\, c(t)dt}{\int_0^\infty c(t)dt} \qquad \textbf{Equation 36}$$

The first moment is an indication of the average time the tracer spends inside the system and the second moment is the variance of the mean residence time.

3.5.3 Porosity Estimation

3.5.3.1 Column Porosity

Porosity characteristics differentiate resin chromatography from membrane chromatography systems. In the context of resin chromatography one can refer to porosity of column or resin, while in membrane chromatography only membrane porosity exists. The different types of porosity for resin chromatography have been reviewed in this section (Schmidt-Traub et al., 2012).

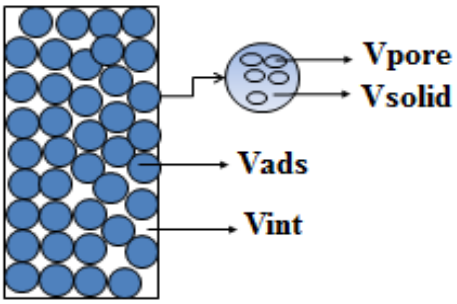

Figure 12: Structure of packed bed system for resin chromatography

Total volume of column, $V_c = V_{ads} + V_{int}$ **Equation 37**

Here V_{ads} is the volume of the adsorbent and V_{int} is the interstitial volume of the fluid phase

Furthermore, $V_{ads} = V_{solid} + V_{pore}$ **Equation 38**

Here V_{solid} is the volume of the solid material of adsorbent and V_{pore} is the volume of pores of adsorbent.

From these volumes different types of porosity can be calculated:

$$\text{Void fraction of column, } \varepsilon_v = \frac{V_{int}}{V_c} \qquad \textbf{Equation 39}$$

$$\text{Porosity of solid phase/adsorbent, } \varepsilon_p = \frac{V_{pore}}{V_{ads}} \qquad \textbf{Equation 40}$$

$$\text{Total porosity of column, } \varepsilon_t = \frac{V_{int} + V_{pore}}{V_c} = \varepsilon_v + (1 - \varepsilon_v)\,\varepsilon_p \qquad \textbf{Equation 41}$$

(Schmidt-Traub et al., 2012) suggested tracer injection to the liquid chromatographic system to determine the total porosity of column and provided the following equation:

$$\varepsilon_t = \frac{t_o\, F'}{V_c} \qquad \textbf{Equation 42}$$

Here F' is the volumetric flow rate during tracer experimentation, t_o is the column dead time and V_c is the total volume of column.

(Altenhoner et al., 1997) used the pulse input method with dextran as tracer to estimate the bed voidage of ion exchange resin according to Equation 43.

$$\varepsilon_r = \frac{\mu\, F'}{V_c} \qquad \textbf{Equation 43}$$

Here F' is the volumetric flow rate during tracer experimentation, μ is the first moment/the mean residence time of tracer and V_c is the total volume of column.

The total porosity of the column (ε_t) and the bed voidage of the resin (ε_r) seem quite comparable from Equation 42 and 43, except that the column dead time is used in Equation 42 and the mean residence time of the tracer is considered in equation 43 which by definition are different.

3.5.3.2 Total porosity of membrane, ε

(Dimartino et al., 2011) determined porosity of membrane column (stacked with multiple affinity membranes) by performing pulse experiment with 40% acetone as the tracer and used the following equation:

$$\varepsilon_m = \frac{\mu F'}{V_{mem}} \qquad \textbf{Equation 44}$$

Here F' is the volumetric flow rate during tracer experimentation, μ is the mean residence time of tracer and V_{mem} is the total membrane volume.

Considering Equations 42-44 the following equation was used in this study to estimate the total porosity of membrane:

$$\varepsilon = \frac{\mu F'}{\frac{\Pi d^2 L}{4}} \qquad \textbf{Equation 45}$$

Here d and L are the outer diameter and thickness of the interior cylinder of the membrane holder respectively (Figure 13).

The porosity evaluated with Equation 45 provides an estimate of the fraction of pores in the membrane.

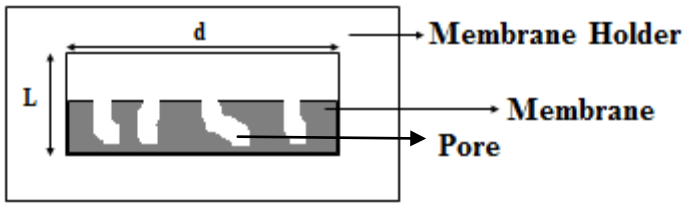

Figure 13: Schematic of the interior of the membrane holder and the membrane pores

It should be noted that instead of taking the external dimensions of the entire membrane holder, the volume of the interior cylinder of the membrane holder was taken. The rationale for this action was that in resin chromatography the resin particles are stacked inside the entire column and in membrane column multiple membranes are stacked inside the entire column. For the membrane holder used in this study one or multiple membranes can be stacked inside the interior cylinder of the membrane holder (Figure 13). So the volume of the interior cylinder of the membrane holder should be taken. However, this approach might be more reasonable and accurate for membrane porosity estimation if multiple membranes are used instead of just one membrane.

Published porosity estimates for ion exchange membrane materials range from 0.5 to 0.95. In these studies membrane porosity has been also termed as membrane void fraction. It can be noted from Table 4 that the reported membranes with porosity values are mostly anion exchangers.

Table 4: Total porosity of ion exchange membranes from literature

Ion Exchange Membrane	Number of membranes inside membrane holder/column	Total porosity of membrane	Determination Method
Anion exchange membrane (Yang & Etzel, 2003)	Stack of seven Q membranes	0.7	Assumption
Mustang Q membrane (Montesinos-Cisneros et al., 2007)	30 membranes	0.7	Assumption
Sartobind™ D MA 75 anion exchanger (Vicente et al., 2008)	15 layers of membrane	0.95	Salt pulse
Sartobind Q anion exchanger (Tatarova et al., 2009)	15 layers of membrane	0.78	Liquid impregnation method
Sartobind D anion exchanger (Vicente et al., 2011)	3 layers of membrane	0.62	Salt pulse
Mustang Q XT5 anion exchanger (Francis et al., 2012; Ghosh et al., 2013)	15 layers of membrane	0.7± 0.05	Manufacturer
Ion Exchange Membrane for simulated modelling (Beijeren et al., 2013)	-	0.7	Assumption
Mustang S cation exchanger (Shekhawat et al., 2016)	-	0.5	Assumption

In some publications, the reported membrane porosity values were taken from the manufacturer (Francis et al., 2012; Ghosh et al., 2013), but no information on the estimation methods was provided. In other publications, membrane porosity values were just mentioned or assumed to perform dynamic modelling (Yang & Etzel, 2003; Montesinos-Cisneros et al., 2007; Beijeren et al., 2013; Shekhawat et al., 2016). Two publications referred to the salt pulse method to estimate membrane porosity (Vicente et al., 2008; Vicente et al., 2011). However, no detail was provided regarding the method. Only (Tatarova et al., 2009) referred to liquid impregnation method to estimate porosity of Sartobind Q and provided basic information about the method.

3.5.4 Interstitial Velocity, U

The interstitial velocity of the mobile phase was calculated as suggested by (Schmidt-Traub et al., 2012; Beijeren et al., 2013):

$$U = \frac{F}{\frac{\varepsilon \Pi d^2}{4}} \qquad \textbf{Equation 46}$$

Here F is the volumetric flow rate during protein binding, Ɛ is the total porosity of membrane (estimated from Equation 45), d and L are the outer diameter and thickness of the interior cylinder of the membrane holder respectively.

3.5.5 Parameters V_{PFR} and D_{ax}

Table 5 presents literature values of V_{PFR} and D_{ax} for membrane chromatography materials along with their determination method, solute investigated (Protein/DNA) and buffer information.

Table 5: Values for V_{PFR} and D_{ax} from literature for membranes

Membrane	Protein/DNA	Buffer	Axial Dispersion Coefficient, D_{ax} (cm^2/s)	Determination Method for D_{ax}	Volume of PFR, V_{PFR} (ml)	Determination Method for V_{PFR}
Anion exchange (Quaternary amine) membrane (Yang & Etzel, 2003)	α- lactalbumin	50 mM Tris (pH 8.3)	$1.1x10^{-6}$	Assumption	2.2	Assumption
	Thyroglobulin	50 mM Tris (pH 8.3)	$2.5x10^{-7}$	Assumption	2.2	Assumption
Mustang Q membrane (Montesinos-Cisneros et al., 2007)	pDNA	TE buffer (pH 8)	$4.56\ X10^{-8}$	$Dax = \frac{6.85\ x10^{-8}\ T}{v\ \sqrt{M^{1/3}R_g}}$ *v* is the viscosity of solute, T is the temperature, M is the molecular weight of solute, R_g is the radius of gyration	0.75-0.90	Assumption
Affinity membrane (B14-TRZ-Epoxy 2) column (Dimartino et al., 2011)	Human IgG	-	-	$Dax = \frac{L'\mu_2}{2\mu^2}\ U$ L' is the membrane stack thickness, μ is the first moment, μ_2 is the second moment, U is interstitial velocity	1.77-2.01	Not mentioned
Mustang Q XT5 anion exchanger (Francis et al., 2012)	Ovalbumin	25 mM Tris-HCl (pH 8)	$0.9\pm0.3\ x10^{-4}$	Assumption	0.38	Assumption
Mustang Q XT5 anion exchanger (Ghosh et al., 2013)	Bovine serum albumin	25 mM Tris-HCl (pH 8)	-	-	2.22	Assumption
Mustang S cation exchanger (Shekhawat et al., 2016)	Monoclonal antibody	15 mM phosphate buffer (pH 6.5)	$4.56x10^{-4}$	Hold up study	-	-

Note: For resin chromatography axial dispersion coefficient is usually estimated by using different empirical correlations (Melter et al., 2008; Osberghaus et al., 2012).

Chapter 4: Materials and Experimental Methods

4.1 Materials

4.1.1 Membranes

Weak cation exchange membranes Natrix C (25 mm diameter) were provided by Natrix Separations Inc. (Burlington, Ontario, Canada). These membranes are macro-porous cross-linked polyacrylate hydrogels containing a high density of carboxylate binding groups physically reinforced by an inert polymeric (polyolefin) mesh (Hassel &Moresoli, 2016; Hou et al., 2015). Strong cation exchange membranes Sartobind S were provided by Sartorius-Stedim (Bohemia, NY, USA) in flat sheet format which were cut into circles of 25 mm diameter (by drawing measured circles on flat sheet membrane) to fit the membrane holder. These membranes are macro-porous stabilised reinforced cellulose membranes with sulfonic acid ligands bound covalently to the complete internal surface of the membrane (Sartobind S A4 Sheet, n.d.).

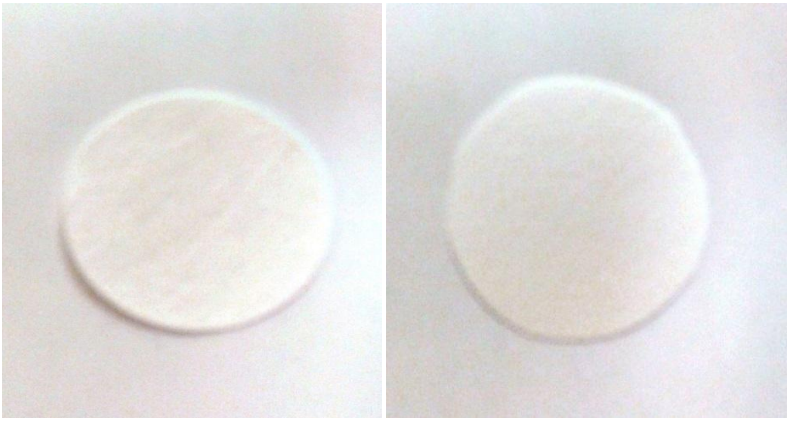

Natrix C **Sartobind S**

Figure 14: Cation exchange membranes used for the experiments

4.1.2 Chemicals

Sodium phosphate citrate buffer (pH 5) was prepared from 0.1M citric acid (anhydrous) (Fisher Scientific, NJ, USA) and 0.2M disodium phosphate (heptahydrate) (Fisher Scientific, NJ, USA). Sodium acetate buffer (pH 5) was prepared from 0.2 M acetic acid (glacial) (Sigma Aldrich, St Louis, MO, USA) and 0.2 M sodium acetate (anhydrous) (Anachemia, Montreal, QC, Canada). Milli- Q water was used during the buffer preparation, obtained from a Millipore synergy water purification system. Acetone solutions of different concentrations were prepared by adding acetone (for hplc, ≥ 99.9%) (Sigma Aldrich, St Louis, MO, USA) in phosphate citrate buffer (pH 5) or acetate buffer (pH 5). 20% Ethanol was prepared from anhydrous Ethanol (Sigma Aldrich, St Louis, MO, USA).

4.1.3 Human IgG

Polyclonal Human IgG was purchased from Equitech-Bio, Inc. (Kerrville, TX, USA).

4.1.4 Membrane holder

The membrane holder used in this study was provided by Natrix Separations Inc. (Burlington, Ontario, Canada). The outer diameter and thickness of the interior cylinder of the membrane holder was measured to be 0.029 m and 0.005 m respectively.

Figure 15: Internal structure of the membrane holder used for the experiments

4.2 Tracer experimentation with acetone

All experiments were performed with the AKTA prime system (Amersham Biosciences, UK) equipped with UV detector and controlled by PrimeView software (Figure 16). Before starting experiment each day, the system was first washed with 20% Ethanol and then with hot deionized water (60^{o}C) for at least 3 times each to have a stable baseline in the chromatogram. The typical washing time with ethanol and hot water each day was around 60 minutes. The acetone solutions were prepared by adding acetone in phosphate citrate buffer (pH 5) or acetate buffer (pH 5) and was mixed in a Multi-purpose Rotator (Thermo Scientific, MA, USA) at 125 rpm for 30 minutes for each experiment.

4.2.1. Acetone calibration

Acetone calibration was developed for the AKTA prime system using 8 different concentrations, 0.5-4% (v/v), by step and pulse input method separately (Appendix A). Each set of eight concentrations was run in triplicates. The absorbance was measured at 280 nm and used to establish a calibration curve between absorbance and acetone concentration following Beer Lambert's law (setting intercept to zero). The membrane holder was not attached to the system when calibration was performed.

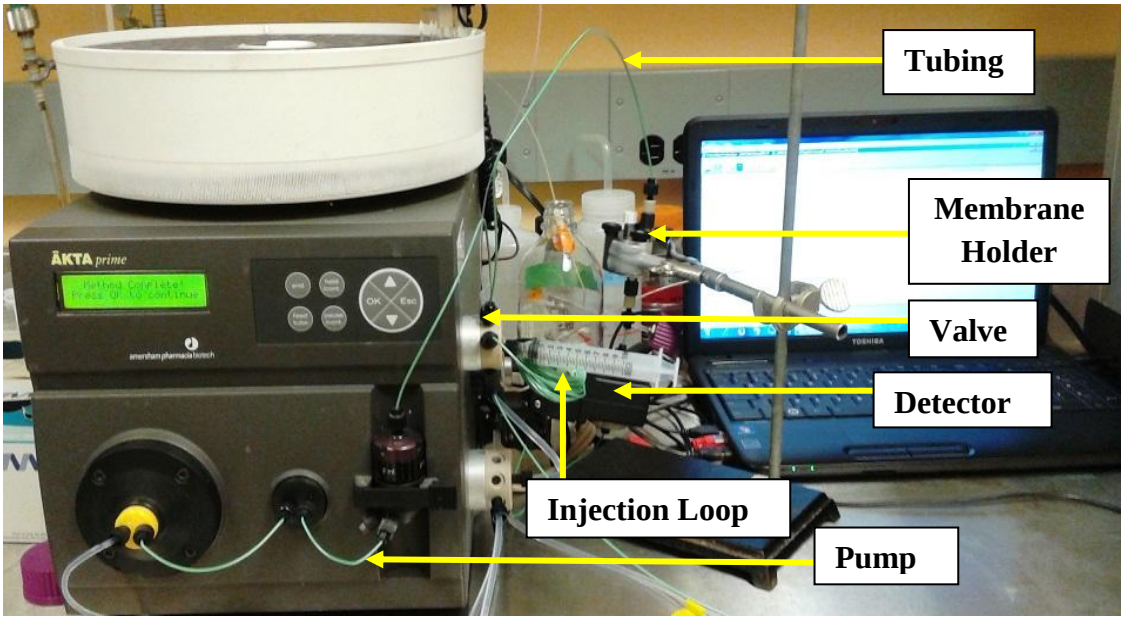

a)

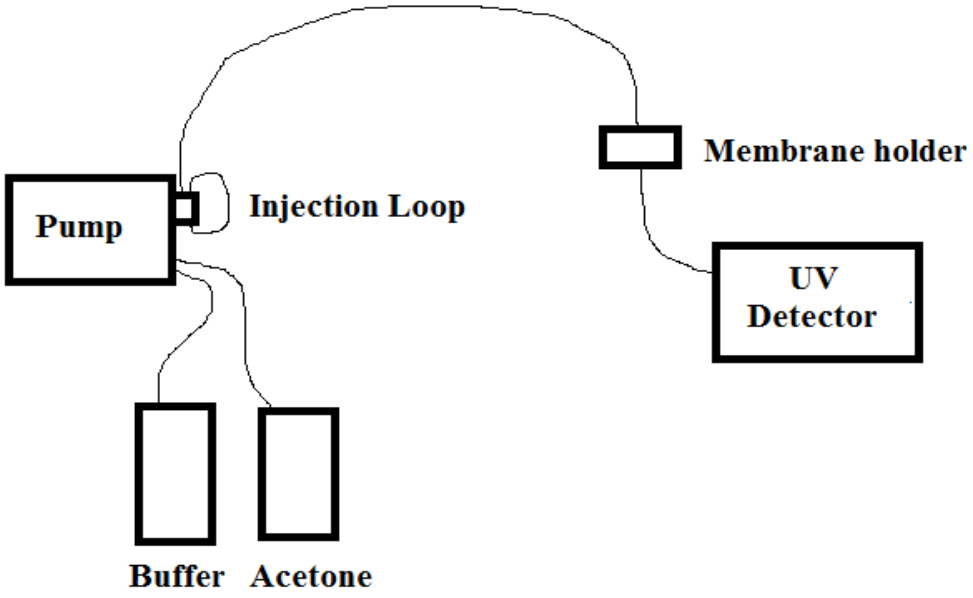

b)

Figure 16: a) AKTA prime system used for experiments b) Schematic of AKTA prime system

4.2.2 Step input tracer method

The system dispersion curves were obtained using step input tracer method. Step input of 1% acetone (v/v) was introduced to the AKTA system for both phosphate citrate buffer (pH 5) and acetate buffer (pH 5) under two conditions, with the membrane holder empty and with one membrane (Natrix C or Sartobind S) in the membrane holder. The flow rate was set as 10 ml/min. During each experiment for first 3 minutes only buffer was run in the system. For next 3 minutes step input of acetone solution was conducted. When the first positive absorbance value of acetone was detected, the overall system volume (V_o) was noted. Finally, the system was washed with buffer for another 3 minutes. Each experiment had a duration of 9 minutes and was performed in triplicates. The first two replicates were executed on the same day, and the 3rd replicate was conducted on a different day to observe how the system responds in different days.

4.2.3 Pulse input tracer method

The total porosity of membrane was estimated by using pulse input tracer method for both phosphate citrate buffer (pH 5) and acetate buffer (pH 5). A pulse of 1% acetone (v/v) was injected into the AKTA prime system at the selected flow rates, 4 ml/min and 10 ml/min flow rate. Before and after acetone injection, 10 ml of buffer was run in the system. Experiments were conducted in triplicates and each replicate was taken on different days. It should be noted that before obtaining each pulse curve, 1% acetone solution was injected in an injection loop manually using a syringe (Figure 16). Then during the experiment the injection of acetone pulse was controlled by the AKTA system.

4.3 Protein binding experiment (dynamic condition)

The experimental data for Immunoglobulin (IgG) binding with Natrix C and Sartobind S membranes using acetate buffer (pH 5) were obtained in the AKTA prime system (Weggen, 2015). IgG binding experiment with phosphate citrate buffer (pH 5) was unsuccessful due to high pressure build-up in the system.

The IgG solution was prepared by dissolving 0.1g of IgG in 200 ml acetate buffer (pH 5) which was mixed in a Multi-purpose Rotator (Thermo Scientific, MA, USA) at 125 rpm for 45 minutes on the day of the experiment to obtain 0.5 mg/ml IgG concentration. A 25 mm

membrane (Natrix C or Sartobind S) was placed in the membrane holder and attached to the AKTA prime system. The membrane was equilibrated with acetate buffer (pH 5) for 10 min at 1 ml/min flow rate. Then the 0.5 mg/ml IgG solution was fed to the system for 100 min at 1 ml/min flow rate to perform protein binding and the absorbance at the outlet of the system was recorded. The absorbance values were then converted to concentration by using the calibration curve for IgG (Appendix A). The IgG concentration at the outlet (C) and the IgG concentration in the feed (C_o) were used to develop breakthrough curves, C/C_o against time of the effluent.

4.4 Statistical analysis using t- test

A t-test is a statistical examination of the average or mean of two population of samples when the sample sizes are small and the variances of the two population are unknown. The sample mean follows a t distribution. The t_{factor} is a tabulated value from t distribution with a particular degree of freedom and significance level of α. When the significance level is α, the confidence level is (1-α) *100%.

In this test, the null hypothesis states that the two sample means are equal to each other, while the alternative hypothesis claims that the sample means are unequal. To verify which hypothesis is correct, a test probe is calculated and compared with the t_{factor}.

If X_1 and ${S_1}^2$ are the mean and variance of the first sample population with n_1 measurements and X_2 and ${S_2}^2$ are the mean and variance of the second sample population with n_2 measurements, then test probe can be written as follows:

$$t_{probe}=\frac{X_1-X_2}{S_p\sqrt{\frac{1}{n_1}+\frac{1}{n_2}}} \qquad \textbf{Equation 47}$$

$$S_p=\frac{(n_1-1){S_1}^2+(n_2-1){S_2}^2}{n_1+n_2-2} \qquad \textbf{Equation 48}$$

When t_{probe} is smaller than or equal to t_{factor} (with degree of freedom of n_1+n_2-2), we cannot reject the null hypothesis, which signifies that the two means are not statistically different from each other. When t_{probe} is greater than t_{factor}, the null hypothesis is rejected and the difference between the two means is statistically significant. In MATLAB the syntax ttest2(x) is used to performed the t-test for x data.

Chapter 5: Overall system volume and total porosity of membrane

5.1 Determination of overall system volume from dispersion curve

As mentioned in chapter 3 (Section 3.2), in a continuous flow system dispersion occurs when some sample molecules diffuse forward ahead of the molar average velocity of the fluid flow, while the others lag behind resulting in a broadening of the sample signal. This phenomenon in a membrane chromatographic system can be evaluated by dispersion curve which represents concentration profile of a non-binding substance called tracer in the outlet of the system.

In this study dispersion curves for AKTA prime system were first obtained without membrane with only membrane holder under two buffer conditions at pH 5 (phosphate citrate buffer and acetate buffer). Then the dispersion curves were obtained by placing one membrane (Natrix C or Sartobind S) inside the membrane holder under two buffer conditions as well. From each dispersion curve the overall system volume, V_o was determined.

For dispersion curve with the empty membrane holder for phosphate citrate buffer (pH 5), Run 1 and 2 were identical. The first acetone concentrations were detected at nearly the same volume, then the acetone concentration increased steadily and the curves leveled off around 1% acetone concentration (Figure 17a). However, Run 3 was quite different (Figure 17a) in the sense that the acetone concentration was detected at a much later volume. In terms of acetate buffer (pH 5), all 3 runs were non-identical for the dispersion curves with the empty membrane holder. The first acetone concentrations were detected at 3 different volumes (Figure 17b).

When dispersion curves were obtained with Natrix C being present in the membrane holder, for both buffers Run 1 and 2 were identical. The acetone concentrations were detected at almost the same volume and the curves were indistinguishable as they overlapped (Figure 18). For Run 3 acetone was again detected nearly at the same volume for both buffers, although the curves shifted slightly, either below (Figure 18a) or above (Figure 18b) the other two curves.

With Sartobind S being present in the membrane holder for both buffers, Run 1 and 2 of the dispersion curves were similar as the acetone concentrations were detected at around the same volumes (Figure 19). However, the dispersion curves for phosphate citrate buffer (pH 5) did not reach around 1% acetone concentration and leveled off at much lower acetone concentrations

(Figure 19a). For Run 3 acetone was again detected nearly at the same volume for phosphate citrate buffer (pH 5), but this time the dispersion curve leveled off around 1% acetone (Figure 19a). For run 3 with acetate buffer (pH 5) the dispersion curve shifted to the right and went over the other two curves (Figure 19b).

Overall the dispersion curves with Natrix C membrane had more stable pattern compared to Sartobind S membrane.

In terms of overall system volume, under two buffer conditions the V_o values with empty membrane holder were not statistically different (α=0.05) from each other (Table 6). Similarly, when a membrane (Natrix C or Sartobind S) was present in the membrane holder, the V_o values were statistically not different (α=0.05) for the two buffers. Details of the t-test analysis (performed with MATLAB) are presented in Appendix B.

While using acetate buffer (pH 5), it seemed that the presence of membrane (Natrix C or Sartobind S) resulted in a higher value for overall system volume (Table 6). However, this observation cannot be confirmed without performing more experiments. Higher number of replicates is required to analyze the precise effect of membrane on the overall system volume.

Note: During obtaining system dispersion curves typically effluent volume is presented in the x-axis instead of time. If these curves need to be compared with protein breakthrough curves, where x-axis generally has time, then the volumes in dispersion curves are converted to time using flow rate.

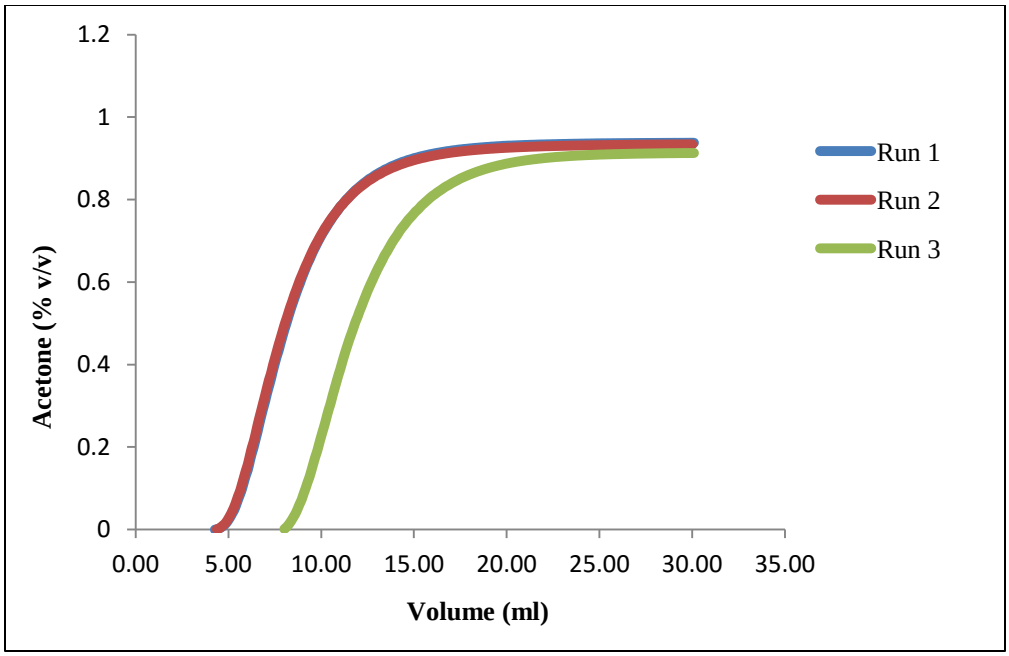

a)

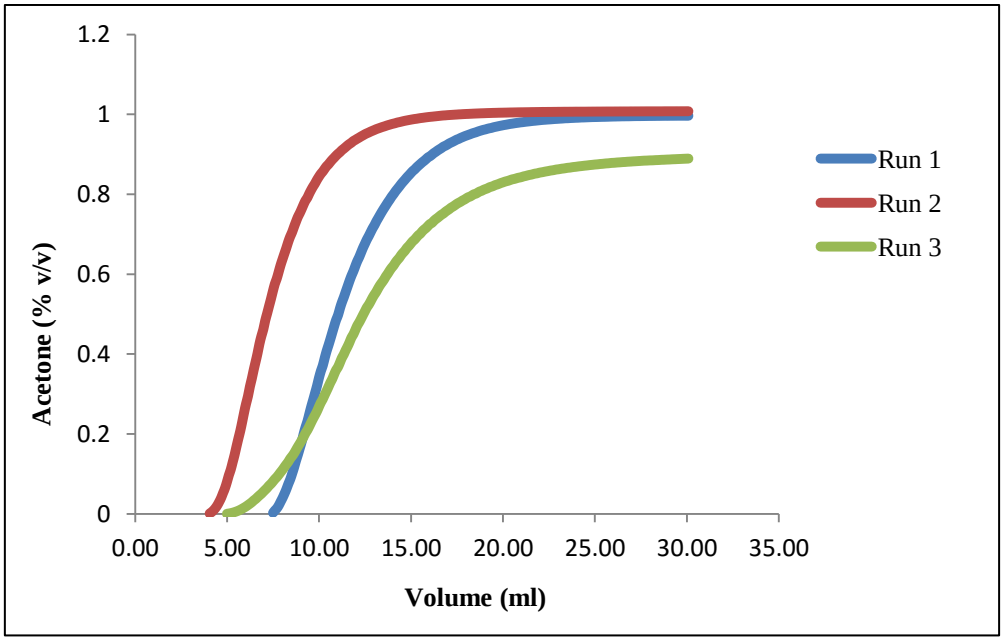

b)

Figure 17: System dispersion curves with empty membrane holder a) phosphate citrate buffer b) acetate buffer

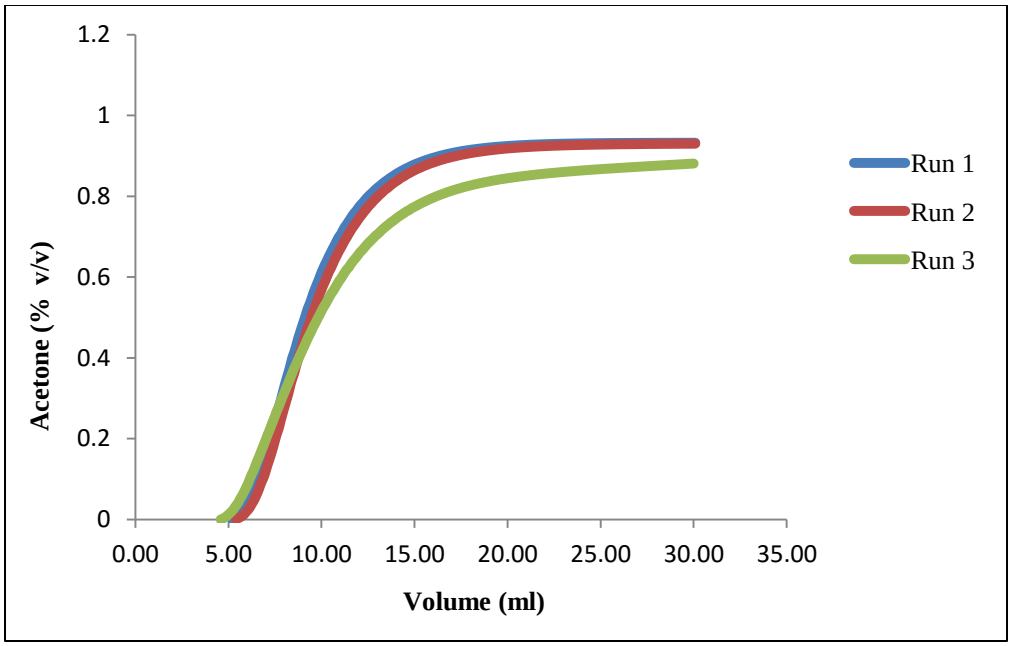

a)

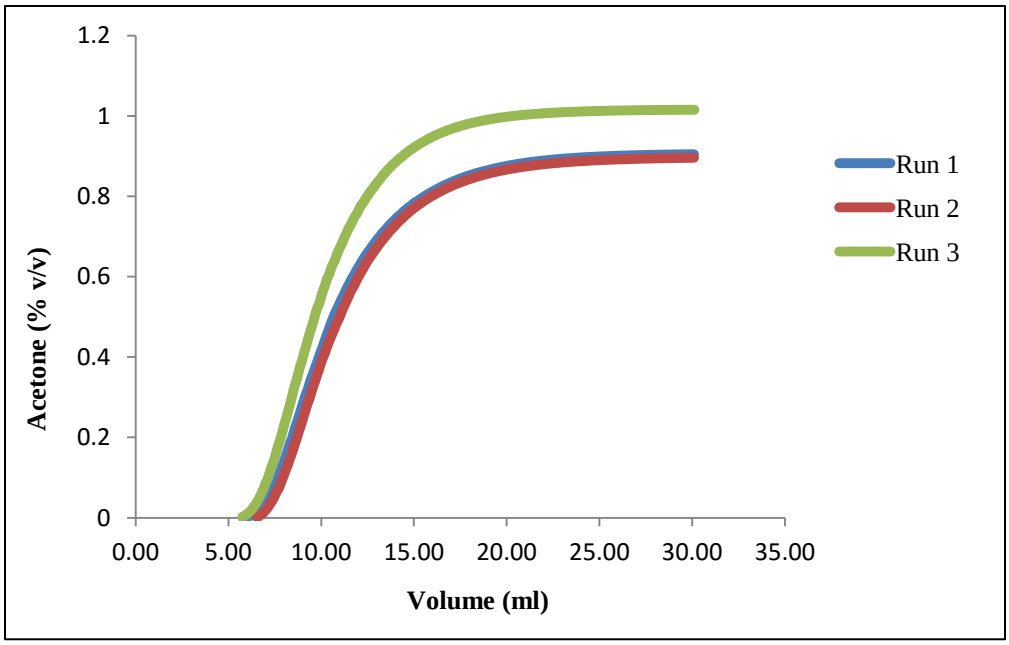

b)

Figure 18: System dispersion curves with Natrix C a) phosphate citrate buffer b) acetate buffer

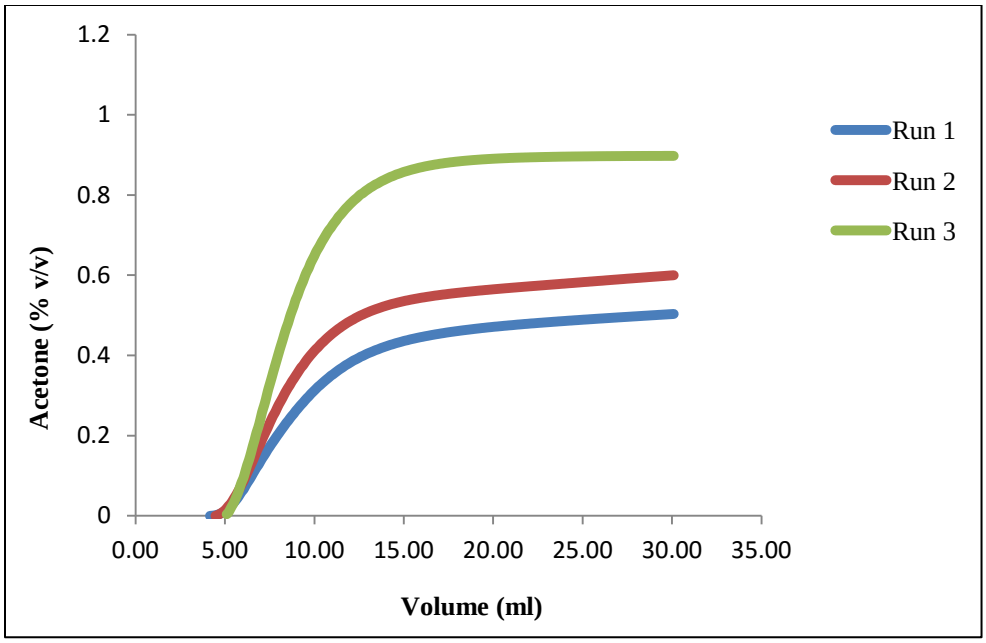

a)

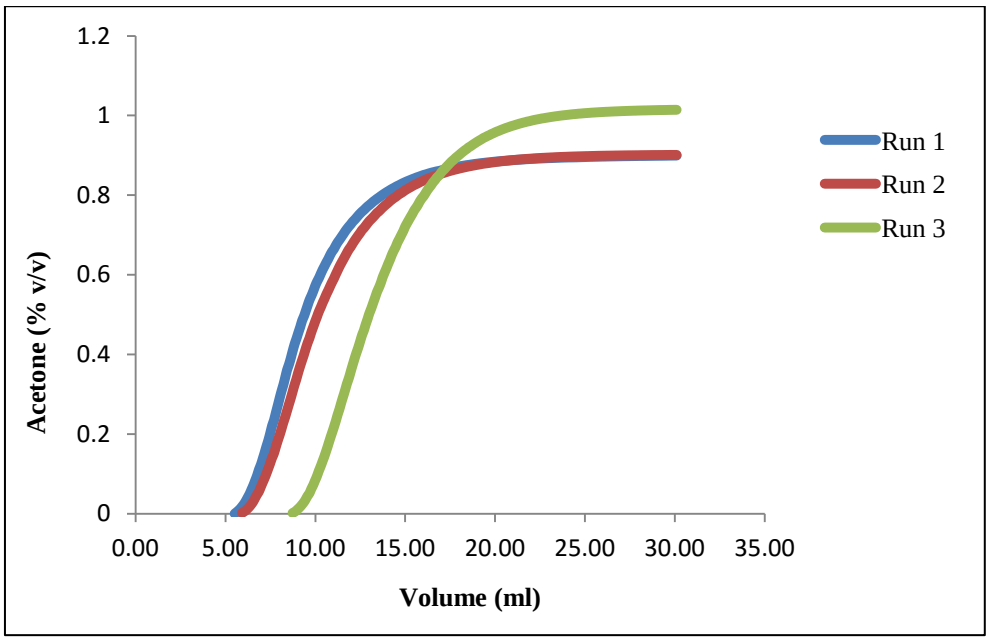

b)

Figure 19: System dispersion curves with Sartobind S a) phosphate citrate buffer b) acetate buffer

Table 6: Overall system volume (V_o) of the AKTA prime system for both buffers

Condition	Phosphate citrate buffer	Acetate buffer
	Overall system volume, V_o (ml)	**Overall system volume, V_o (ml)**
Without membrane (empty membrane holder)	5.55±2.13	5.51±1.77
With Natrix C	5.06±0.43	6.04±0.45
With Sartobind S	4.58 ± 0.58	6.73± 1.76

*V_o values are presented as (average± standard deviation) calculated from 3 replicates.

5.2 Determination of total porosity of membrane and interstitial velocity from Pulse curve

While placing one membrane (Natrix C or Sartobind S) inside the membrane holder, 1% acetone pulse was injected into the AKTA system at two different flow rates (4 ml/min and 10 ml/min) under two buffer conditions at pH 5 (phosphate citrate buffer and acetate buffer). The pulse data were used to determine mean residence time, μ (Equation 35), total porosity of membrane, Ɛ (Equation 45) and interstitial velocity (Equation 46).

It was noted that for a specific flow rate the shapes of the pulse curves were different for each replicate (Figure 20 and 21). However, the values for the areas under the curves were pretty similar even though the shapes were different. Since determination of mean residence time, μ involves solving two integrations in numerator and denominator (Equation 35), area under the curve is more important than the shape of the curve. The pulse curves for 4 ml/min were shifted to the right compared to the curves for 10 ml/min (Figure 20 and 21).

The total porosity estimates of Natrix C membrane with the phosphate citrate buffer (pH 5) were statistically (α= 0.05) similar at the two flow rates (Table 7). For the porosity estimation with acetate buffer (pH 5) for Natrix C, it seemed like the values were highly different from each other for the two flow rates (Table 7). However, statistically they were found not to be significantly different (α= 0.05). Similar to Natrix C, the porosity estimation for Sartobind S with phosphate citrate buffer (pH 5) were statistically (α= 0.05) similar at the two flow rates (Table 7). However, for Sartobind S and acetate buffer (pH 5), the porosity values at two flow rates were found to be statistically (α= 0.05) different from each other (Table 7).

Details of the porosity calculation and t-test analysis (performed with MATLAB) are presented in Appendix C and D respectively.

In terms of interstitial velocity, for both membranes the higher the porosity the lower the interstitial velocity, which was expected according to Equation 46.

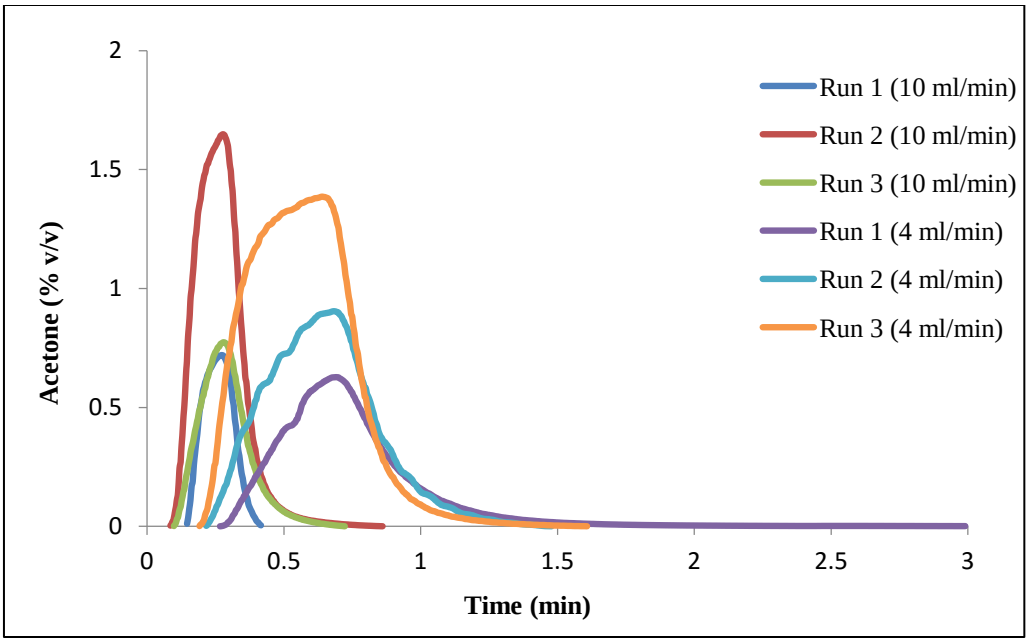

a)

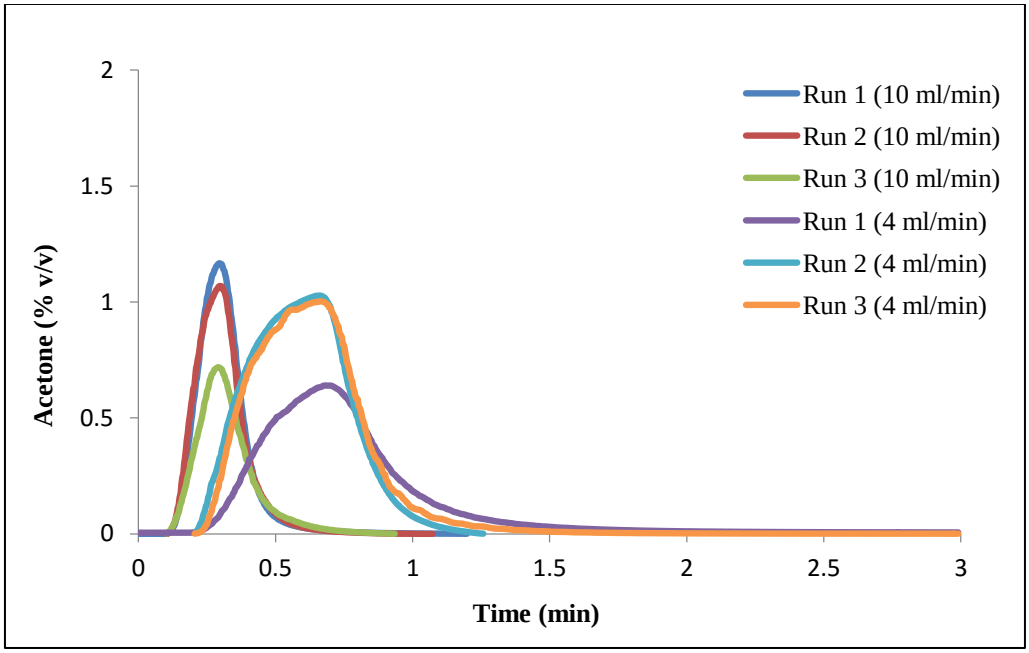

b)

Figure 20: Pulse runs at different flow rates for Natrix C a) phosphate citrate buffer b) acetate buffer

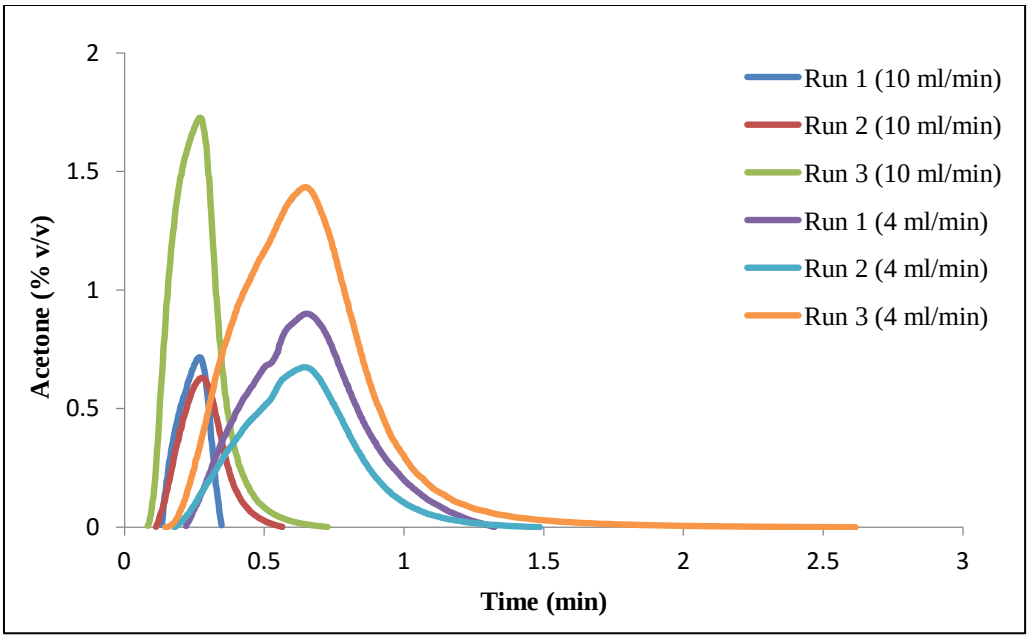

a)

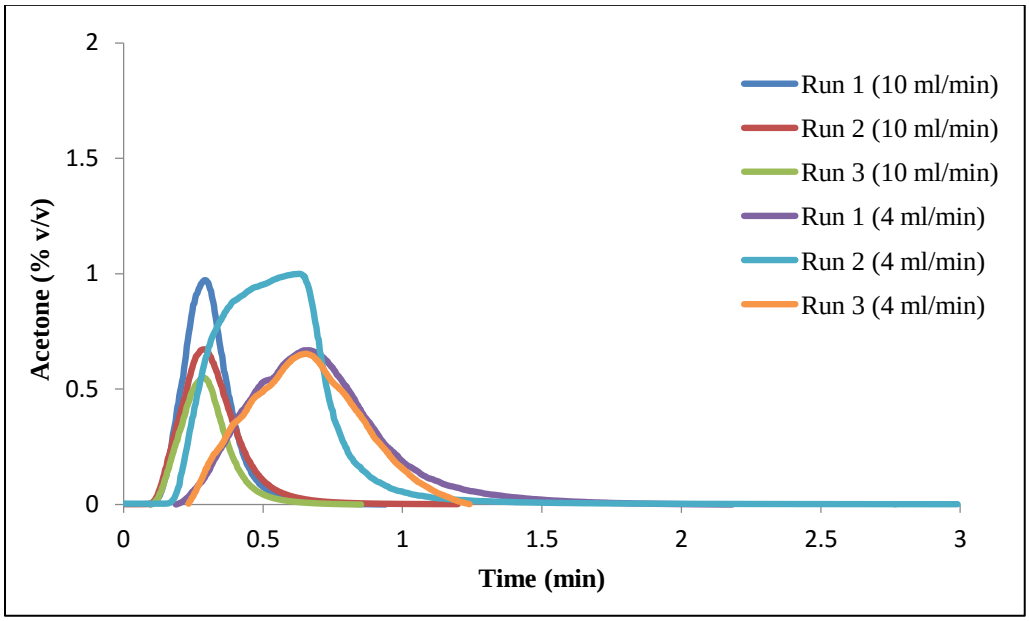

b)

Figure 21: Pulse runs at different flow rates for Sartobind S a) phosphate citrate buffer b) acetate buffer

Table 7: Mean residence time, total porosity of membrane and interstitial velocity

Type of Membrane	Type of Buffer	Flow rate, F' (ml/min)	Mean residence time, μ (min)	Total porosity of membrane, ε	Interstitial velocity, U (m/s)
Natrix C	Phosphate citrate	10	0.27±0.02	0.82±0.04	$3.07x10^{-5} \pm 1.59x10^{-6}$
		4	0.65±0.09	0.79±0.10	$3.25x10^{-5} \pm 4.20x10^{-6}$
	Acetate	10	0.31±0.01	0.95±0.03	$2.67x10^{-5} \pm 7.94x10^{-7}$
		4	0.66±0.09	0.80±0.11	$3.18x10^{-5} \pm 4.24x10^{-6}$
Sartobind S	Phosphate citrate	10	0.26±0.02	0.80±0.06	$3.19x10^{-5} \pm 2.35x10^{-6}$
		4	0.65±0.01	0.79±0.02	$3.20x10^{-5} \pm 7.57x10^{-7}$
	Acetate	10	0.31±0.01	0.94±0.03	$2.69x10^{-5} \pm 8.54x10^{-7}$
		4	0.64±0.08	0.77±0.09	$3.30x10^{-5} \pm 4.35x10^{-6}$

*μ, ε and U values are presented as (average± standard deviation) calculated from 3 replicates.

5.3 Discussion

5.3.1 Overall system volume

In the current study, 1% acetone (v/v) dissolved in either phosphate citrate buffer (pH 5) or acetate buffer (pH 5) was used as tracer in the AKTA prime system to obtain the dispersion curves using Natrix C (non-wet volume 0.135 ml) and Sartobind S (non-wet volume 0.118 ml) cation exchange membranes. During obtaining dispersion curves one membrane was placed inside the membrane holder being connected to the AKTA prime system and a flow rate of 10 ml/min was used. From the system dispersion curves overall system volume, V_o was determined when first positive absorbance value of acetone was noted in the outlet. The overall system volume takes into account the dead volumes from the membrane system as well as the external system (Section 3.4.1).

As mentioned in Table 6, with Natrix C being present in the membrane holder the V_o values were 5.06± 0.43 ml and 6.04±0.45 ml for phosphate citrate buffer (pH 5) and acetate buffer (pH 5) respectively, which were statistically (α=0.05) not different from each other. With Sartobind S being present in the membrane holder, the V_o values were 4.58± 0.58 ml and 6.73± 1.76 ml for phosphate citrate buffer (pH 5) and acetate buffer (pH 5) respectively, which were also not statistically (α=0.05) different from each other.

Comparatively in literature, (Teepakorn et al., 2015) obtained system dispersion curve for AKTA prime-plus chromatographic system using phosphate buffer containing 5% acetone (v/v) as the tracer at 12 Bed Volume/min flow rate. The experiments were conducted with Sartobind S75 and Sartobind Q75 membrane devices, which are strong cation exchanger (with sulfonic acid groups) and strong anion exchanger (with quaternary ammonium groups) respectively. The devices contained stabilized reinforced cellulose membrane in a stack of 15 membrane discs, where each device had a membrane bed volume (BV) of 2.1 ml. With Sartobind S75 or Q75 device being connected to the AKTA prime-plus system, Teepakorn and colleagues measured dead volume of the device and the external system (denoted as V_o) when outlet acetone concentration reached 10% of its initial concentration and determined the dead volumes to be 6.06 ml for both Sartobind devices (Teepakorn et al.,2015).

The overall system volume values obtained experimentally from this study ranged in between 4.5 ml to 6.80 ml for both membranes and the V_o values from literature were within this range. Therefore, the results obtained from this study were comparable to those in literature.

5.3.2 Total porosity of membrane and interstitial velocity

For Natrix C membrane, the porosity estimates using pulse of 1% acetone were in the range of 0.79-0.95 and for Sartobind S membrane the range was 0.77-0.94, which are similar to the values from literature (Table 4). It was interesting to note that for phosphate citrate buffer (pH 5) both membranes exhibited similar porosity values for two different flow rates (Table 7). However, effect of flow rate was observed during the porosity estimation with acetate buffer (pH 5) for both membranes.

The mean residence time, μ was higher at 10 ml/min for acetate buffer (pH 5) than phosphate citrate buffer (pH 5) for both membranes. For instance, at 10 ml/min with Natrix C membrane, μ was 0.31±0.01 min with acetate buffer (pH 5) and 0.27±0.02 min with phosphate citrate buffer (pH 5). At 10 ml/min with Sartobind S membrane, μ was 0.31±0.01 min with acetate buffer (pH 5) and 0.26±0.02 min with phosphate citrate buffer (pH 5). But at 4 ml/min flow rate mean residence time with both buffers were similar for both membranes (Table 7). Therefore, at 10 ml/min flow rate in the presence of acetate buffer (pH 5), the higher mean residence time resulted in higher porosity estimation for both membranes. At this point no precise explanation can be provided regarding this experimental observation without exploring the effect of a range of flow rates on the porosity estimation using acetate buffer (pH 5) with larger number of replicates.

(Dimartino et al., 2011) used Equation 44 to determine porosity of affinity membrane column using 40% acetone as the tracer. The estimated porosity value with tracer was 0.545±0.068, which was compared with porosity obtained using a different method called mercury intrusion porosimetry (Dimartino et al., 2011). The porosity value obtained with mercury intrusion porosimetry was 0.585 (Dimartino et al., 2011). The consistent results from the two methods suggested that the membrane porosity estimation using tracer is a valid method.

In terms of the validity of the method used in this study, as mentioned earlier the porosity estimation using Equation 45 would be more accurate if a stack of membranes was used instead of one membrane inside the membrane holder. Therefore, for the improvement of the pulse input tracer method for porosity estimation, the use of a stack of membrane is highly imperative.

For interstitial velocities, the values were in the range of 2.60×10^{-5} m/s to 3.30×10^{-5} m/s for both membranes under both buffer conditions (Table 7). As mentioned earlier with increasing porosity, the interstitial velocity decreased in all cases. For instance, with Natrix C and acetate buffer (pH 5), for porosity 0.95±0.03 the interstitial velocity was $2.67 \times 10^{-5} \pm 7.94 \times 10^{-7}$ m/s and for porosity 0.80±0.11 the interstitial velocity was $3.18 \times 10^{-5} \pm 4.24 \times 10^{-6}$ m/s.

Note: For hydrogel membranes, (Beijeren et al., 2013) mentioned that the total porosity of membrane includes transport pores in the membrane through which the protein solution passes as well as the pores of the hydrogel layer (Figure 1). Since the Natrix C membrane is a hydrogel membrane, it was assumed that the estimated porosity of Natrix C included both transport pores and hydrogel pores.

Chapter 6: Dynamic modelling for cation exchange membrane chromatography

6.1 Unknown model parameter estimation

The dynamic modelling involved known as well as unknown parameters which are presented in Figure 22. The modelling was performed in 3 steps for both Natrix C and Sartobind S membrane in MATLAB using the "PDEPE" and "LSQNONLIN" solvers.

"PDEPE" solver in MATLAB solves systems of partial differential equations (PDE) in space variable x and time t by converting the PDEs into ordinary differential equations (ODE) by spatial discretization. The time integration is performed with ODE15s, which is a built in function in MATLAB for solving ordinary differential equations. The algorithm in "LSQNONLIN" solver solves non-linear least square problems by using trust region reflective method. This method chooses a trusted region (ellipsoidal) around current search point and within this region a quadratic model is minimized.

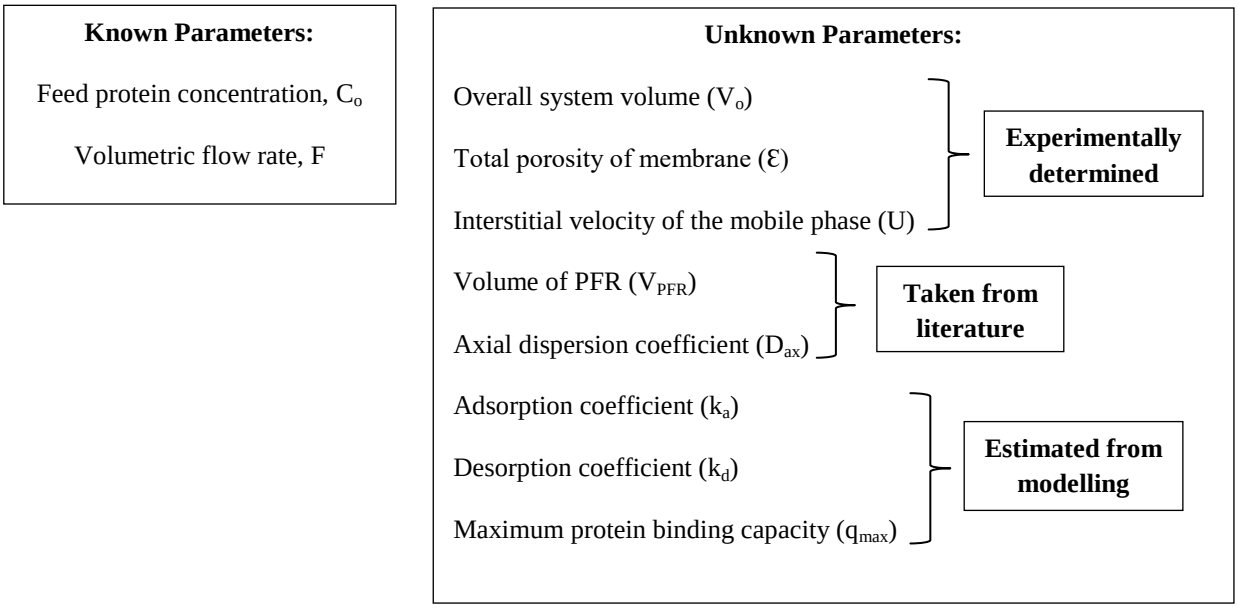

Figure 22: The known and unknown model parameters for dynamic modelling

6.1.1 First step of modelling

In the first step the 3 Langmuir parameters (k_a, k_d, q_{max}) (Equation 19) were estimated by fitting the model breakthrough curve to the experimental breakthrough curve through minimizing sum of squared error (SSE). During this fitting the other parameters (C_o, F, V_o, Ɛ, U, V_{PFR}, D_{ax}) remained constant. The experimental breakthrough curves for IgG binding with both membranes were obtained with acetate buffer (pH 5) (Section 4.3). The initial values for k_a and q_{max} were taken from literature (Yang & Etzel, 2003; Hassel, 2015; Niu, 2015) and k_d was chosen randomly (Table 8).

The values for C_o and F were taken from the experimental conditions (Section 4.3). The V_o values were experimentally determined as 6.04 ml with the presence of Natrix C and 6.73 ml with Sartobind S using acetate buffer (pH 5) (Table 6). V_{PFR} and D_{ax} values were taken from literature (Yang & Etzel, 2003). In terms of total porosity of membrane, during tracer experiment with acetate buffer (pH 5) two mean Ɛ values were obtained for both Natrix C and Sartobind S. For Natrix C the Ɛ values were 0.95 and 0.80, and for Sartobind S the Ɛ values were 0.94 and 0.77 (Table 7). Each porosity value corresponded to one interstitial velocity value. During first step of modelling, both porosities along with their respective interstitial velocities were chosen as input parameters. A summary of the input parameters is presented in Table 9.

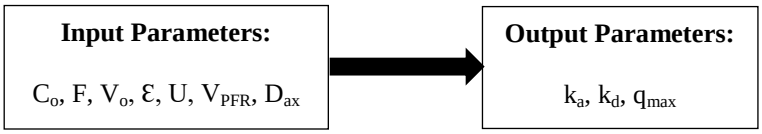

Figure 23: Input and output parameters for first step of dynamic modelling

6.1.2 Second step of modelling

In the second step of modelling total porosity of membrane was estimated along with the 3 Langmuir parameters. The purpose of this was to compare the porosity values obtained through tracer experiments to those estimated from modelling. The initial conditions for the estimated parameters and the input parameters for the second step of modelling are presented in Table 10 and 11 respectively.

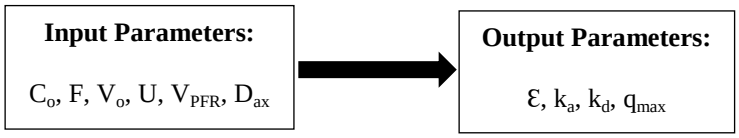

Figure 24: Input and output parameters for second step of dynamic modelling

6.1.3 Third step of modelling

Finally, the sensitivity of the parameter total porosity of membrane, Ɛ was analyzed for both Natrix C and Sartobind S membranes. The porosity value was increased by 5% for each membrane to evaluate the effect on the Langmuir parameters k_a, k_d and q_{max}.

Table 8: Initial values for estimation of Langmuir parameters (1st part)

Parameters	Membrane	
	Natrix C	Sartobind S
Adsorption coefficient, k_a (ml/mg.s)	13.20×10^{-2}	13.20×10^{-2}
Desorption Coefficient, k_d (s^{-1})	10×10^{-2}	10×10^{-2}
Maximum protein binding capacity, q_{max} (mg/ml)	214	41

Table 9: Input parameters for dynamic modeling (1st part)

Parameters	Membrane	
	Natrix C	Sartobind S
Feed concentration of protein, C_o (mg/ml)	0.5	0.5
Volumetric flow rate during protein binding, F (ml/min)	1	1
Overall system volume (V_o) (ml)	6.04	6.73
Total porosity of membrane (ε)	0.95 and 0.80	0.94 and 0.77
Interstitial velocity of the mobile phase (U) (m/s)	2.67×10^{-5} and 3.18×10^{-5}	2.69×10^{-5} and 3.30×10^{-5}
Volume of PFR, V_{PFR} (ml)	2.2	2.2
Axial dispersion coefficient, D_{ax} (m^2/s)	1.1×10^{-10}	1.1×10^{-10}

Table 10: Initial values for estimation of Langmuir parameters and total porosity of membrane (2nd part)

Parameters	Membrane	
	Natrix C	Sartobind S
Adsorption coefficient, k_a (ml/mg.s)	13.20×10^{-2}	13.20×10^{-2}
Desorption Coefficient, k_d (s^{-1})	10×10^{-2}	10×10^{-2}
Maximum protein binding capacity, q_{max} (mg/ml)	214	41
Total porosity of membrane (Ɛ)	0.80	0.77

Table 11: Input parameters for dynamic modeling (2nd part)

Parameters	Membrane	
	Natrix C	Sartobind S
Feed concentration of protein, C_o (mg/ml)	0.5	0.5
Volumetric flow rate during protein binding, F (ml/min)	1	1
Overall system volume (V_o) (ml)	6.04	6.73
Interstitial velocity of the mobile phase (U) (m/s)	3.18×10^{-5}	3.30×10^{-5}
Volume of PFR, V_{PFR} (ml)	2.2	2.2
Axial dispersion coefficient, D_{ax} (m^2/s)	1.1×10^{-10}	1.1×10^{-10}

6.2 Modelling results

For the first step of modelling, the fit between the model and experimental breakthrough curve for IgG binding with Natrix C was very good for the two porosity estimates (Figure 25), resulting in similar SSE value of 0.07. However, the fit between the model and experimental breakthrough curve was not very good for Sartobind S (Figure 26) as the SSE value was 20.47 for both porosity values. The estimated Langmuir parameters for each case are presented in Table 12.

For the second step of modelling with Natrix C membrane, the fit between the model and experimental breakthrough curve was also very good, while for Sartobind S once again the fit was inadequate (Figure 27). The SSE values for model fitting with Natrix C and Sartobind S were also 0.07 and 20.47 respectively. The estimated Langmuir parameters as well as the porosities of both membranes are presented in Table 13.

In the final step during parameter sensitivity analysis, it was observed that with increasing porosity for Natrix C, the q_{max} values increased steadily (Figure 28). The k_a and k_d values remained constant within a certain porosity range. After porosity of around 0.93, the k_a values started to increase, while the k_d values started to decrease (Figure 28). However, neither of the changes was very prominent. The porosity sensitivity analysis with Sartobind S was unsuccessful due to inadequate model fitting. No specific pattern was observed in the Langmuir parameters while increasing the porosity values (Figure 29).

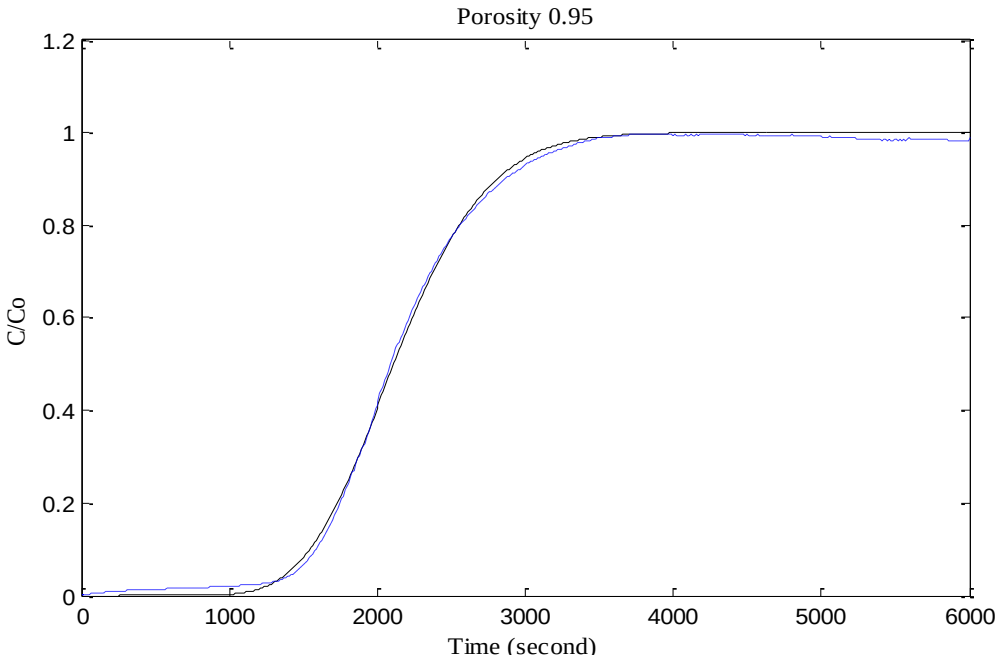

a)

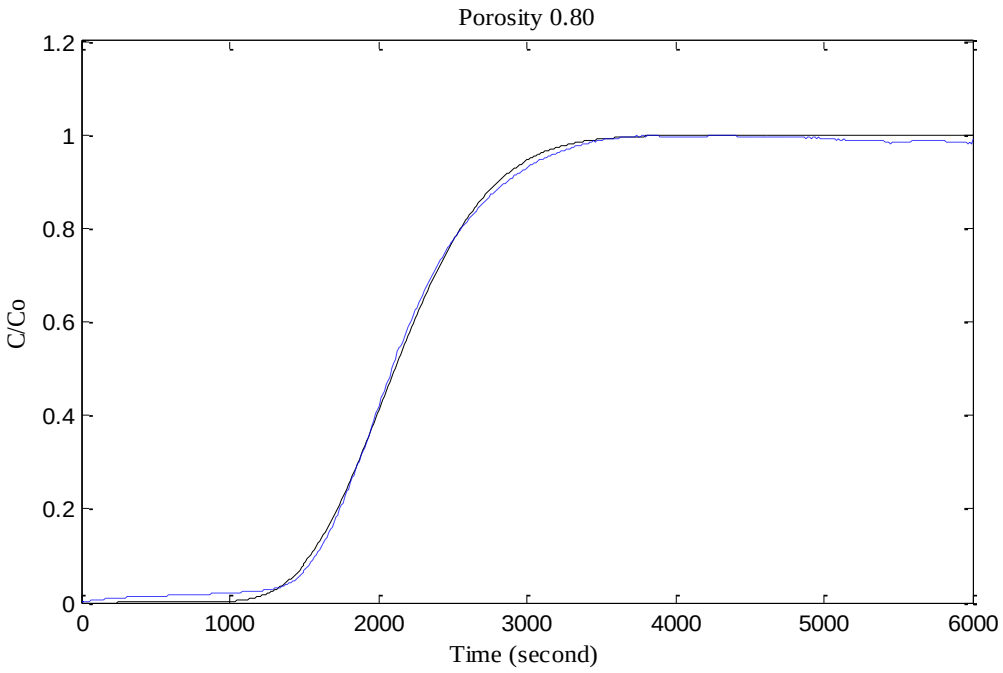

b)

Figure 25: IgG breakthrough curves with Natrix C for a) porosity 0.95 and b) porosity 0.80

(Blue dotted line experimental curve, Black solid line model curve)

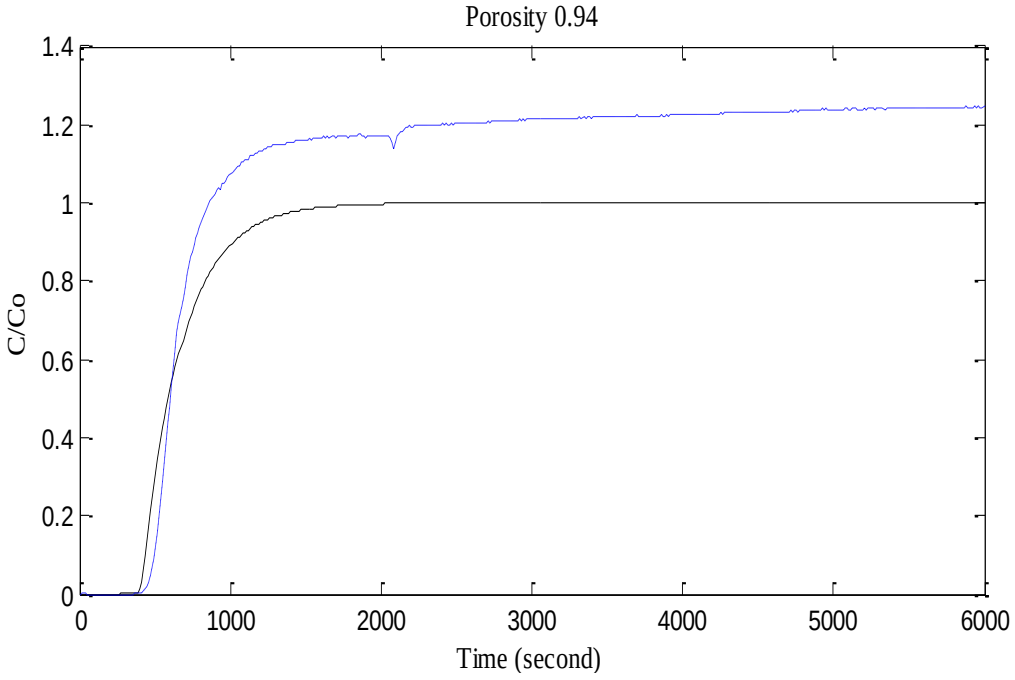

a)

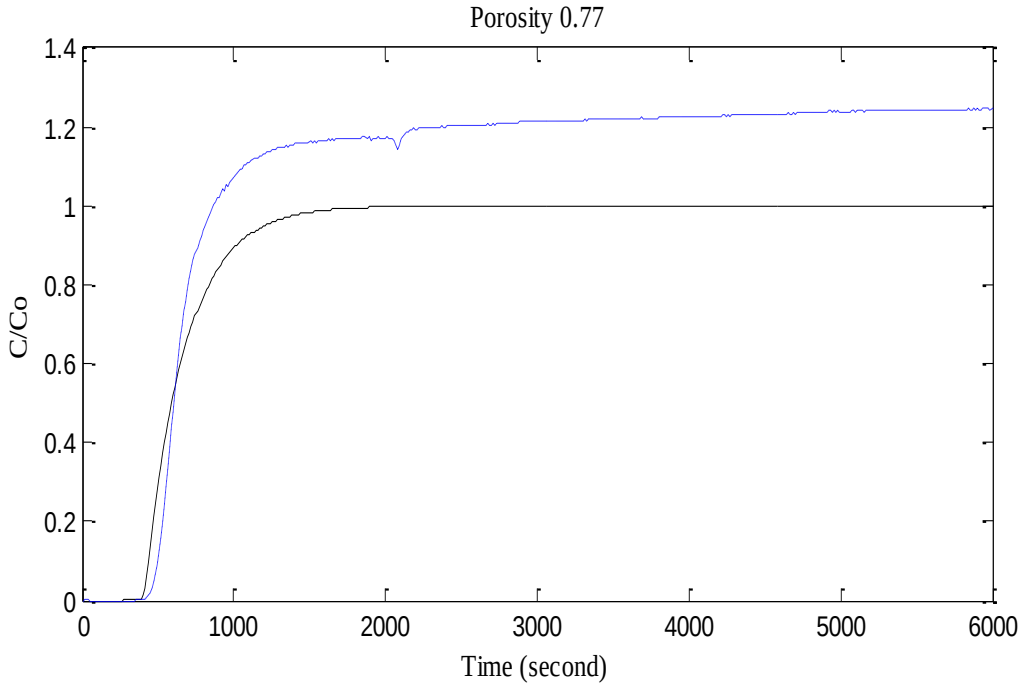

b)

Figure 26: IgG breakthrough curves with Sartobind S for a) porosity 0.94 and b) porosity 0.77

(Blue dotted line experimental curve, Black solid line model curve)

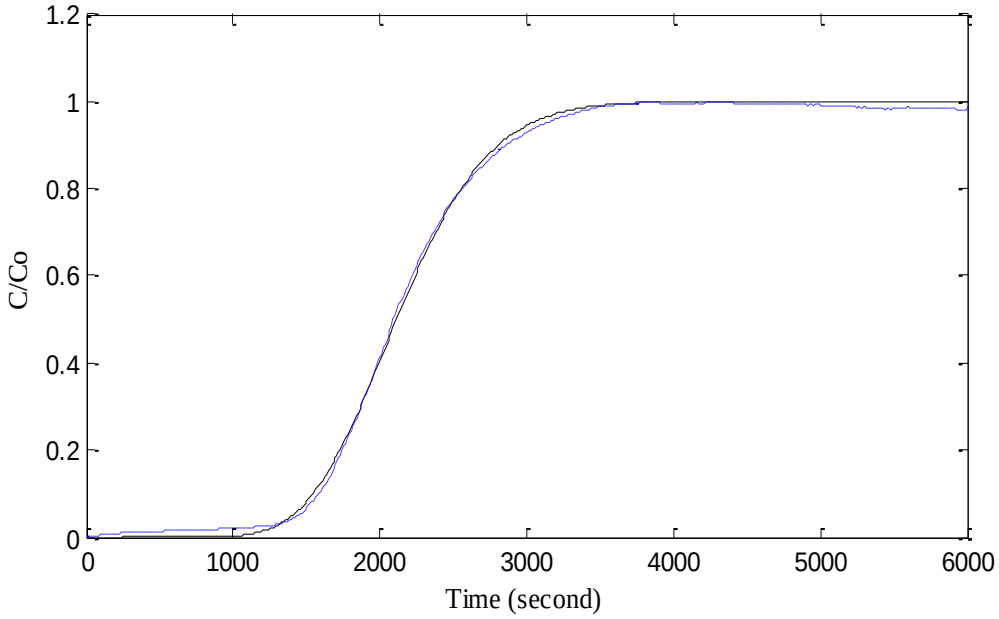

a)

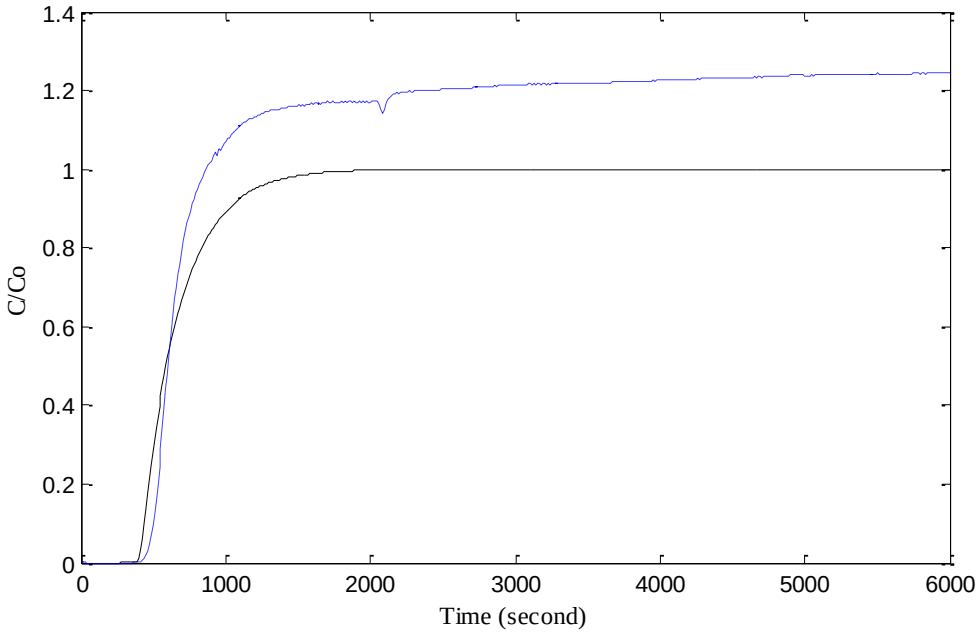

b)

Figure 27: IgG breakthrough curves for estimating Langmuir parameters and porosity with a) Natrix C and b) Sartobind S

(Blue dotted line experimental curve, Black solid line model curve)

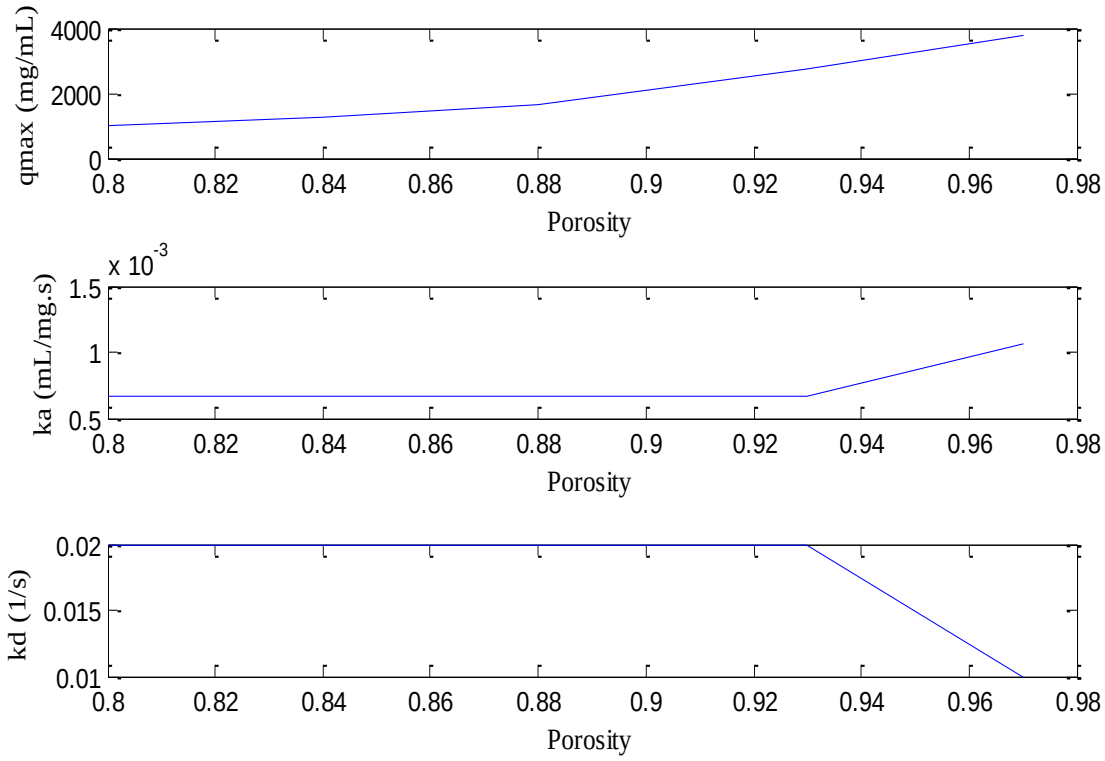

Figure 28: Parameter Sensitivity analysis for Natrix C

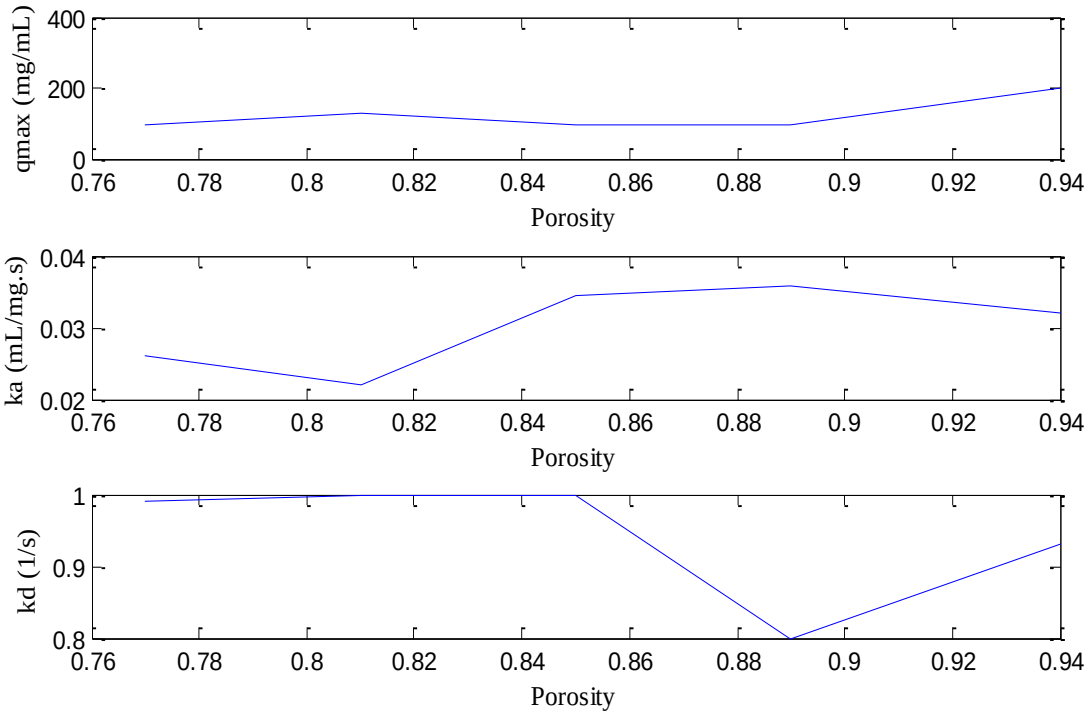

Figure 29: Parameter Sensitivity analysis for Sartobind S

Table 12: Estimated Langmuir parameters and comparison with literature

Parameters	Natrix C		Sartobind S		Mustang Q XT5 (Francis et al., 2012)	Mustang Q XT5 (Ghosh et al., 2013)
	Ɛ= 0.95	Ɛ =0.80	Ɛ= 0.94	Ɛ= 0.77	Ɛ= 0.70±0.05	Ɛ= 0.70±0.05
Adsorption coefficient, k_a (ml/mg.s)	9.33×10^{-4}	6.67×10^{-4}	3.92×10^{-2}	3.10×10^{-2}	5.12×10^{-3}	6.4×10^{-2}
Desorption coefficient, k_d (s^{-1})	2×10^{-2}	2×10^{-2}	77×10^{-2}	97×10^{-2}	1.1×10^{-3}	6×10^{-3}
Maximum protein binding capacity, q_{max} (mg/ml)	2800	1008	136.5	82.5	373	284.04

Table 13: Estimated Langmuir parameters and total porosity of membrane

Parameters	Natrix C	Sartobind S
Adsorption coefficient, k_a (ml/mg.s)	6.67×10^{-4}	1.67×10^{-2}
Desorption coefficient, k_d (s^{-1})	2×10^{-2}	78×10^{-2}
Maximum protein binding capacity, q_{max} (mg/ml)	1011	120
Total porosity of membrane (Ɛ)	0.80	0.77

6.3 Discussion

6.3.1 Natrix C and Langmuir model parameter estimates

The estimated Langmuir parameters from the first step of modelling varied according to input porosity values. It can be noted from Table 12 that for porosity 0.95 the k_a value was $9.33x10^{-4}$ ml/mg.s and q_{max} was 2800 mg/ml, while for porosity 0.80 the k_a value decreased to $6.67x10^{-4}$ ml/mg.s and q_{max} decreased to 1008 mg/ml. It was interesting to observe that with decreasing porosity both k_a and q_{max} decreased. The k_d value was $2x10^{-2}$ s^{-1} for both porosities.

In Natrix C the hydrogel layers containing the carboxylate functional groups fill the pores of the membrane. Since membrane porosity is considered proportional to the volume of pores (Tatarova et al., 2009), it can be stated that the higher the porosity, the higher the pore volume. When pore volume is higher, proteins can have better access to the binding sites leading to increased protein adsorption. This phenomenon can explain the proportional relation of adsorption coefficient and maximum protein binding capacity with porosity.

For the second step of modelling the Langmuir parameters were estimated along with the total porosity of membrane. It was noticed that the k_a and k_d were again $6.67x10^{-4}$ ml/mg.s and $2x10^{-2}$ s^{-1} respectively (Table 13). Maximum protein binding capacity, q_{max} was estimated to be 1011 mg/ml, while porosity remained the same as the initial value of 0.80 (Table 10 &13). Thus, the modelling was not able to estimate porosity value different from the initial value, which means that experimental determination of membrane porosity is a more valid approach.

6.3.2 Sartobind S and Langmuir model parameter estimates

The estimated Langmuir parameter estimates from the first step of modelling were also affected by porosity for Sartobind S. For porosity 0.94 the k_a value was $3.92x10^{-2}$ ml/mg.s and q_{max} was 136.5 mg/ml, while for porosity 0.77 the k_a value decreased to 3.10 $x10^{-2}$ ml/mg.s and q_{max} decreased to 82.5 mg/ml (Table 12). Once again a proportional relation was observed between the porosity and adsorption coefficient and maximum protein binding capacity. This time an increase in k_d value was observed with decreasing porosity, $77x10^{-2}$ s^{-1} for porosity 0.94 and $97x10^{-2}$ s^{-1} for porosity 0.77 (Table 12).

In Sartobind S membrane sulfonic acid ligands cover the interior areas of the pores. Once again it can be stated that the higher porosity corresponding to higher pore volume leads to increased access of proteins to the binding sites, resulting in better adsorption and binding capacity. When porosity is decreased, the access of proteins to binding sites is reduced, which can indirectly lead to increased value of desorption coefficient.

From the second step of modelling for Sartobind S, the values of k_a, k_d, q_{max} and ε were estimated as 1.67×10^{-2} ml/mg.s, 78×10^{-2} s^{-1}, 120 mg/ml and 0.77 respectively (Table 13). Once again, the porosity value was same as the initial value and the model was unable to estimate a different porosity value (Table 10 & 13).

However, the estimated parameters in both steps of modelling cannot be considered valid due to inadequate model fitting with Sartobind S. In the experimental breakthrough curve of IgG binding with Sartobind S, the maximum value of C/C_o was higher than 1 (Figure 26, 27b). Although the actual reason behind this pattern was not clear, several assumptions were made. It is possible that during the binding step the proteins got detached from the membrane and flowed out through the outlet. If this is indeed the case then it means that the protein binding efficiency of Sartobind S is not very high.

It is also possible that discrepancy observed during the calibration with IgG could cause C/C_o to go over 1. The absorbance values in the AKTA system fluctuated a lot. For one day the 0.5 mg/ml IgG concentration corresponded to one absorbance value, while the next day it corresponded to a completely different absorbance value. The variant absorbance values might be actually accountable for C/C_o going over 1. However, extensive troubleshooting of the AKTA system is required to confirm this assumption.

6.3.3 Comparison of Langmuir model parameter estimates with published studies of ion exchange membranes

(Francis et al., 2012) used Mustang Q XT5 anion exchange membrane capsule (Pall, Inc., East Hills, NY), containing modified hydrophilic polyethersulfone (PES) membranes, to perform breakthrough experiments with protein ovalbumin using 25 mM Tris-HCl (pH 8) buffer. Since the membrane was anion exchanger, the pH of the binding buffer was over the isoelectric point (4.5) of ovalbumin (Ovalbumin, 2015) which would result in negative charge on protein surface. The initial protein concentration was 1 mg/ml, flow rate was 5 ml/min and the experiments were performed in AKTA explorer system (Francis et al., 2012). (Ghosh et al., 2013) also used Mustang Q XT5 anion exchange membrane capsule to obtain breakthrough curve with protein Bovine serum albumin (BSA) using 25 mM Tris buffer (pH 8). The pH of the binding buffer was chosen over the isoelectric point (5.4) of BSA (Shi et al., 2005). During experiment in AKTA explorer system the initial protein concentration was 1mg/ml and flow rate was 12 Column Volume/min.

In this study, the IgG binding experiments with cation exchange membranes Natrix C and Sartobind S were performed in AKTA prime system using acetate buffer (pH 5). Since the membranes were cation exchangers, the pH of the binding buffer was chosen below the isoelectric point (6.5-10) of IgG (Wrzosek & Polakovic, 2011). The initial protein concentration was 0.5 mg/ml and flow rate was 1 ml/min during protein binding.

Compared to literature Natrix C resulted in much higher estimates for maximum protein binding capacity, q_{max} with IgG. Francis and colleagues estimated q_{max} for ovalbumin to be 373 mg/ml and Ghosh and colleagues estimated q_{max} for BSA to be 284.04 mg/ml with Mustang Q XT5 anion exchange membrane which had a porosity of 0.70 ± 0.05 (Table 12). In this study, the estimated q_{max} values for IgG binding with Natrix C were 2800 mg/ml (ε= 0.95) and 1008 mg/ml (ε =0.80) (Table 12). Since the reported porosity of Mustang Q XT5 is lower than Natrix C, it could have contributed to lower estimates for maximum protein binding capacity.

While the estimated adsorption coefficients (k_a) for IgG binding with Natrix C were lower, the desorption coefficients (k_d) were higher compared to literature (Table 12). The model fitting

resulted in a SSE value of 0.07, which was much less than the reported SSE value of 1.249 by (Francis et al., 2012).

However, it should be noted that ovalbumin (molecular weight 42.7 kDa) (Ovalbumin, 2015) and BSA (molecular weight 66.41 kDa) (Shi et al., 2005) have lower molecular weight than IgG, which has a molecular weight of 150 kDa (Antibody Basics, n.d.). If molecular weight is considered equivalent to size, then IgG is much larger molecule than ovalbumin and BSA. Since Langmuir model is more applicable for smaller proteins, the Langmuir parameter estimates for ovalbumin and BSA might be more valid than IgG.

For Sartobind S since the model fitting was inadequate, the estimated Langmuir parameters were not quite comparable with the parameter estimates from literature.

Chapter 7: Comparison between Natrix C and Sartobind S

From the system dispersion curves obtained for two types of pH 5 buffer (phosphate citrate buffer and acetate buffer) with the presence of membrane, it was noted that the curves with Natrix C had more stable pattern compared to Sartobind S. It is possible that the hydrogel layers in the pores of the Natrix C membrane contributed in stabilizing the liquid flow. However, no specific comment can be made without analyzing the internal structures of the membranes in detail. In terms of porosity values obtained under two buffer conditions and two different flow rates, both membranes exhibited similar values. For Natrix C the porosity ranged from 0.79-0.95, while for Sartobind S the porosity ranged from 0.77-0.94.

When IgG binding experiments with both membranes were performed at the presence of acetate buffer (pH 5), the breakthrough curve with Natrix C was more consistent compared to Sartobind S. During IgG binding with Natrix C, the C/C_o values of the breakthrough curve stabilized around the value of 1 indicating that the membrane was properly saturated with IgG during the binding step. However, during IgG binding with Sartobind S, the C/C_o values of the breakthrough curve went over the value of 1 which was undesirable. This could have occurred either due to IgG detachment from the membrane during the binding step or calibration discrepancy. In either case, the IgG binding experiment with Sartobind S was unsuccessful and needs to be further investigated to identify the exact source of error.

Since the experimental breakthrough curve with Natrix C was stable, the model fitting was good with very small SSE value of 0.07. This made the Langmuir parameters estimated from modelling with Natrix C valid and comparable with the parameters estimated in literature. Similarly, as the breakthrough curve with Sartobind S was unstable, the model fitting was inadequate with high SSE value of 20.47. Therefore, the estimated Langmuir parameters using Sartobind S were not very accurate and comparable with literature. From parameter sensitivity analysis a proportional relation between total porosity of membrane and maximum protein binding capacity was clearly observed for Natrix C. However, for Sartobind S the parameter sensitivity analysis was unsuccessful.

Therefore, Natrix C membrane in general exhibited better performance compared to Sartobind S membrane.

Chapter 8: Conclusions and Recommendations

The primary objective of this study was to perform dynamic modelling of cation exchange membrane chromatography for capturing antibody IgG. Two commercial cation exchange membranes Natrix C and Sartobind S were used for the experiments. The modelling consisted of solving three differential equations explaining the protein mass conservation, the protein adsorption (Langmuir model) and the system dispersion. These equations contained total 8 model parameters, three of these parameters (V_o, ε and U) were determined from tracer experiments using 1% acetone as the tracer.

The overall system volume, $V_{o,}$ was determined from the system dispersion curves obtained by step input tracer method under two buffer conditions for each membrane. The difference between V_o values determined with phosphate citrate buffer (pH 5) and acetate buffer (pH 5) was not significant for with and without membrane conditions.

The total porosity of membrane, ε was determined from pulse curves obtained by pulse input tracer method for two different flow rates (10 ml/min and 4 ml/min) under two buffer conditions. During porosity estimation with phosphate citrate buffer (pH 5), change of flow rate didn't have any prominent effect on porosity values for both membranes. But with acetate buffer (pH 5) at 10 ml/min flow rate, the porosity estimates were higher for both membranes. However, it is not very clear what might be actually contributing to this effect without performing more detailed tracer experiments.

Experimental data for IgG binding with Natrix C and Sartobind S membranes using acetate buffer (pH 5) were used to perform dynamic modelling. The model IgG breakthrough curve resulted in good fitting for Natrix C, but the fitting was inadequate for Sartobind S. The parameter sensitivity analysis of Natrix C indicated that the porosity had a proportional relation with the maximum protein binding capacity. This information can lead to designing membranes with optimum porosity.

Overall, the objective of this study was successfully fulfilled, although with some limitations. The results that were positive created the opportunity to extend further research in the area of dynamic modelling of cation exchange membrane chromatography. Most importantly, the

porosity estimation of cation exchange membranes using pulse input tracer method was a novel contribution.

To improve the limitations of this study and aid in future research the following actions are highly recommended:

- For more accurate porosity estimation a stack of membrane should be used instead of just one membrane inside the membrane holder. The similarity or difference in porosity using one membrane and a stack of membrane should be analyzed more carefully. Additionally, mercury intrusion porosimetry is recommended to be used to estimate the porosity of Natrix C and Sartobind S. The porosities obtained with mercury intrusion porosimetry should be compared with those obtained from tracer method to verify the accuracy and validity of tracer method.
- At the presence of acetate buffer (pH 5) the effect of flow rate on membrane porosity should be further investigated. The AKTA prime system can handle flow rate as high as 20 ml/min. Thus, a range of flow rates, from 2 ml/min to 20 ml/min, is recommended to be evaluated for porosity estimation using tracer method with larger number (>3) of replicates.
- Experimentation with IgG and Sartobind S using acetate buffer (pH 5) and calibration with IgG should be further investigated to evaluate why C/C_o values of breakthrough curve go beyond 1.
- Protein adsorption in the dynamic modelling should be analyzed with Steric Mass Action (SMA) model to obtain more extensive understanding about adsorption mechanism by including protein size and charge effects.

References

Altenhoner, U., Meurer, M., Strube, J., & Schmidt-Traub, H. (1997). Parameter estimation for the simulation of liquid chromatography. *Journal of Chromatography A, 769*, 59-69.

Antibody Basics. (n.d.). Retrieved from Sigma-Aldrich: http://www.sigmaaldrich.com/technical-documents/articles/biology/antibody-basics.html

Beijeren, P. V., Kreis, P., & Zeiner, T. (2013). Development of a generic process model for membrane adsorption. *Computers and Chemical Engineering, 53*, 86-101.

Beijeren, P.V., Kreis, P., & Zeiner, T. (2012). Ion exchange membrane adsorption of bovine serum albumin- Impact of operating and buffer conditions on breakthrough curves. *Journal of Membrane Science, 415-416*, 568-576.

Boi, C. (2007). Membrane adsorbers as purification tools for monoclonal antibody purification. *Journal of Chromatography B, 848*, 19-27.

Boi, C., Dimartino, S., & Sarti, G. C. (2007). Modelling and simulation of affinity membrane adsorption. *Journal of Chromatography A,, 1162*, 24-33.

Brooks, C. A., & Crammer, S. M. (1992). Steric Mass-Action Ion Exchange: Displacement Profiles and Induced Salt Gradients. *AlChE, 38*(12), 1969-1978.

Charcosset, C. (1998). Purifications of Proteins by Membrane Chromatography. *J. Chem. T echnol. Biotechnol., 71*, 95-110.

Chen, W. D., Hu, H. H., & Wang, Y. D. (2006). Analysis of steric mass-action model for protein adsorption equilibrium onto porous anion-exchange adsorbent. *Chemical Engineering Science, 61*, 7068-7076.

Dimartino, S., Boi, C., & Sarti, G. C. (2011). A validated model for the simulation of protein purification through affinity membrane chromatography. *Journal of Chromatography A, 1218*, 1677-1690.

Dimartino, S., Boi, C., & Sarti, G. C. (2015). Scale-up of affinity membrane modules: comparison between lumped and physical models. *J. Mol. Recognit., 28*, 180-190.

Fogler, S. H. (2006). *Elements of Chemical Reaction Engineering* (4th ed.). Pearson Education, Inc.

Fractogel EMD SO3 (M). (n.d.). Retrieved May 19, 2015, from EMD Millipore: http://www.emdmillipore.com/CA/en/product/Fractogel%C2%AE-EMD-SO%E2%82%83%E2%81%BB-%28M%29,MDA_CHEM-116882?CatalogCategoryID=

Fractogel EMD TMAE (M). (n.d.). Retrieved May 19, 2015, from EMD Millipore: http://www.emdmillipore.com/CA/en/product/Fractogel%C2%AE-EMD-TMAE-%28M%29,MDA_CHEM-116881?CatalogCategoryID=

Francis, P., Lieres, E. V., & Haynes, C. (2012). Zonal Rate Model for Stacked Membrane Chromatography Part II: Characterizing Ion-Exchange Membrane Chromatography Under Protein Retention Conditions. *Biotechnology and Bioengineering, 109*(3), 615-629.

Ghosh, P., Vahedipour, K., Lin, M., Vogel, J. H., Haynes, C. A. & Lieres, E.V. (2013). Zonal Rate Model for Axial and Radial Flow Membrane Chromatography. Part I: Knowledge Transfer Across Operating Conditions and Scales. *Biotechnology and Bioengineering, 110*(4).

Ghosh, R. (2002). Protein separation using membrane chromatography: opportunities and challenges. *Journal of Chromatography A, 952*, 13-27.

Hassel, K. (2015). *Protein Capture by Cation Exchange Membranes.* PhD Thesis, University of Waterloo, Chemical Engineering.

Hassel, K., & Moresoli, C. (2016). Role of pH and Ionic strength on weak cation exchange microporous Hydrogel membranes and IgG capture. *Journal of Membrane Science, 498*, 158-166.

Hofer, S., Ronacher, A., Horak, J., Graalfs, H., & Lindner, W. (2011). Static and dynamic binding capacities of human immunoglobulin G on polymethacrylate based mixed-modal, thiophilic and hydrophobic cation exchangers. *Journal of Chromatography A, 1218*, 8925-8936.

Hou, Y., Brower, M., & Pollard, D. (2015). Advective Hydrogel Membrane Chromatography for Monoclonal Antibody Purification in Bioprocessing. *Biotechnol. Prog., 31*(4).

Melter, L., Butte, A., & Morbidelli, M. (2008). Preparative weak-cation exchange chromatography of monoclonal antibody variants I. single-component adsorption. *Journal of Chromatography A, 1200*, 156-165.

Mohan, C. (2003). *Buffers: A guide for the preparation and use of buffers in biological system*. Retrieved March 2016, from http://home.sandiego.edu/~josephprovost/Calbiochem_Buffers_Booklet.pdf

Montesinos-Cisneros, R. M., Olivas, J., Ortega, J., Guzman, R., & Tejeda-Mansir, A. (2007). Breakthrough Performance of Plasmid DNA on Ion Exchange Membrane Columns. *Biotechnol. Prog, 23*, 881-887.

Muller, E. (2005). Properties and Characterization of High Capacity Resins for Biochromatography. *Chem.Eng.Technol., 28*(11), 1295-1305.

Niu, H. (2015). *Effect of Buffer on Protein Capture with Weak Cation Exchange Membranes.* Masters Thesis, University of Waterloo, Chemical Engineering.

Nozawa, S. R., Rigoli, I. C., Thedei, & Rossi, A. (n.d.). *Mind the buffering capacity of citric acid*. Retrieved March 2016, from http://www.fgsc.net/fgn42/nozawa.html

Orr, V., Zhong, L., Moo-Young, M., & Chou, C. P. (2013). Recent advances in bioprocessing application of membrane chromatography. *Biotechnology Advances, 31*, 450-465.

Osberghaus, A., Hepbildikler, S., Nath, S., Haindl, M., Lieres, E. V., & Hubbuch, J. (2012). Determination of parameters for the steric mass action model- A comparison between two approaches. *Journal of Chromatography A, 1233*, 54-65.

Ovalbumin. (2015). Retrieved from Worthington: http://www.worthington-biochem.com/oa/default.html

Phosphate Buffers. (n.d.). Retrieved March 2016, from http://www.chem.fsu.edu/chemlab/Mastering/PhosphateBuffers.htm

Sartobind Q Single Step. (n.d.). Retrieved May 19, 2015, from Sartorius: http://www.sartorius.com/en/product/product-detail/92iexq42d9-ss-a/

Sartobind S A4 Sheet. (n.d.). Retrieved May 21, 2015, from Sartorius: http://www.sartorius.com/en/product/product-detail/94iexs42-001/

Saxena, A., Tripathi, B. P., Kumar, M., & Shahi, V. K. (2009). Membrane-based techniques for the separation and purification of proteins: An overview. *Advances in Colloid and Interface Science, 145*, 1-22.

Schmidt-Traub, H., Schulte, M., & Seidel- Morgenstern, A. (2012). *Preparative Chromatography* (2nd ed.). Wiley VCH.

Shekhawat, L. K., Manvar, A. P., & Rathore, A. S. (2016). Enablers for QbD implementation: Mechanistic modeling for ion-exchange membrane chromatography. *Journal of membrane science, 500*, 86-98.

Shi, Q., Ying, Z., & Sun, Y. (2005). Influence of pH and Ionic Strength on the Steric Mass Action Model Parameters around the Isoelectic point of Protein. *Biotechnol. Prog, 21*(2), 516-523.

Tatarova, I., Faber, R., Denoyel, R., & Polakovic, M. (2009). Characterization of pore structure of a strong anion-exchange membrane adsorbent under different buffer and salt concentration conditions. *Journal of Chromatography A, 1216*, 941-947.

Teepakorn, C., Fiaty, K., & Charcosset, C. (2015). Optimization of lactoferrin and bovine serum albumin separation using ion-exchange membrane chromatography. *Separation and Purification Technology, 151*, 292-302.

Vicente, T., Faber, R., Alves, P.M., & Carrondo, M.J.T.(2011). Impact of Ligand Density on the Optimization of Ion-Exchange Membrane Chromatography for Viral Vector Purification. *Biotechnology and Bioengineering, 108*(6), 1347-1359.

Vicente, T., Sousa, M. F.Q., Peixoto, C., Mota, J. P.B., Alves, P. M., & Carrondo, M. J. T.(2008). Anion-exchange membrane chromatography for purification of rotavirus-like particles. *Journal of Membrane Science, 311*, 270-283.

Weggen, T. J. (2015). *Investigation and optimization of interaction between Human IgG and weak cation exchange membranes.* Bachelor's Thesis, Karlsruhe Institute of Technology.

Wrzosek, K., & Polakoviˇc, M. (2011). Effect of pH on protein adsorption capacity of strong cation exchangers with grafted layer. *Journal of Chromatography A, 1218*, 6987– 6994.

Wrzosek, K., Acai, P., Gramblicka, M., & Polakovic, M. (2013). Modeling of equilibrium and kinetics of human polyclonal immunoglobulin G adsorption on a tentacle cation exchanger. *Chemical Papers, 67*(12), 1537-1547.

Yang, G., Bai, L., Yan, C., Gu, Y., & Ma, J. (2011). Preparation of a strong-cation exchange monolith by a novel method and its application in the separation of IgG on high performance liquid chromatography. *Talanta, 85,* 2666-2672.

Yang, H., & Etzel, M. R. (2003). Evaluation of three kinetic equations in models of protein purification using ion-exchange membranes. *Ind.Eng. Chem. Res., 42*, 890-896.

Yang, H., Bitzer, M., & Etzel, M. R. (1999). Analysis of Protein Purification Using Ion-Exchange Membranes. *Ind. Eng. Chem. Res., 38*(10), 4044-4050.

APPENDICES

Appendix A: Calibration Graphs

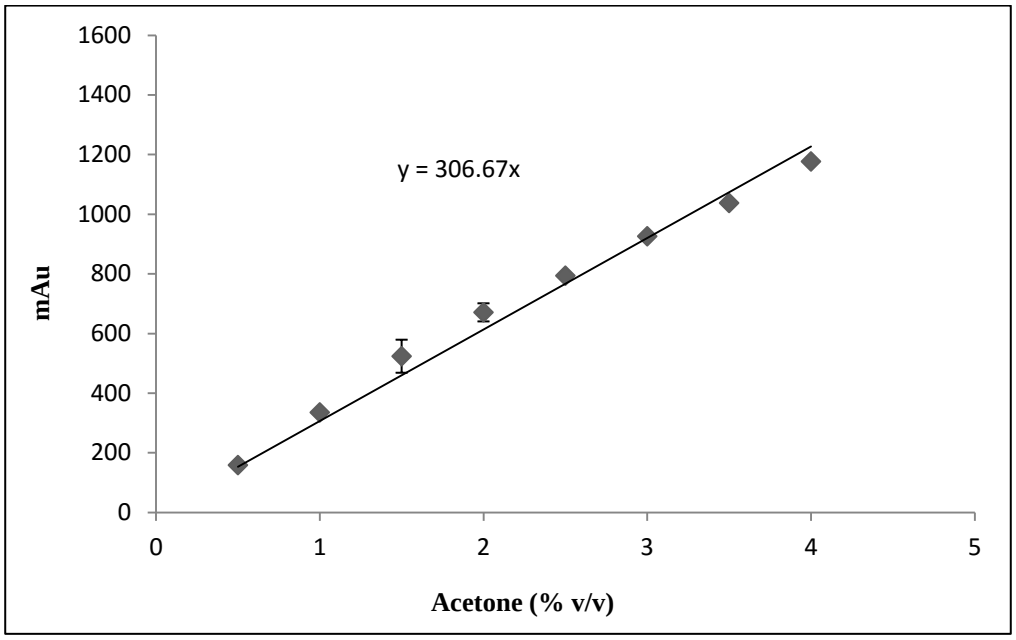

a)

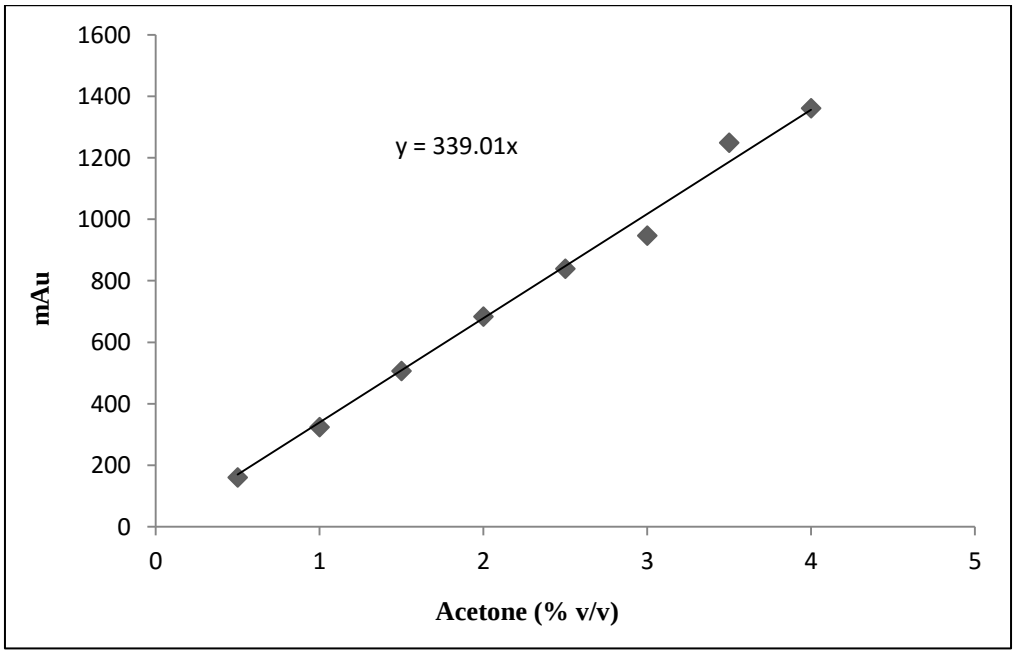

b)

Figure 30: Acetone calibration using step input method a) phosphate citrate buffer b) acetate buffer

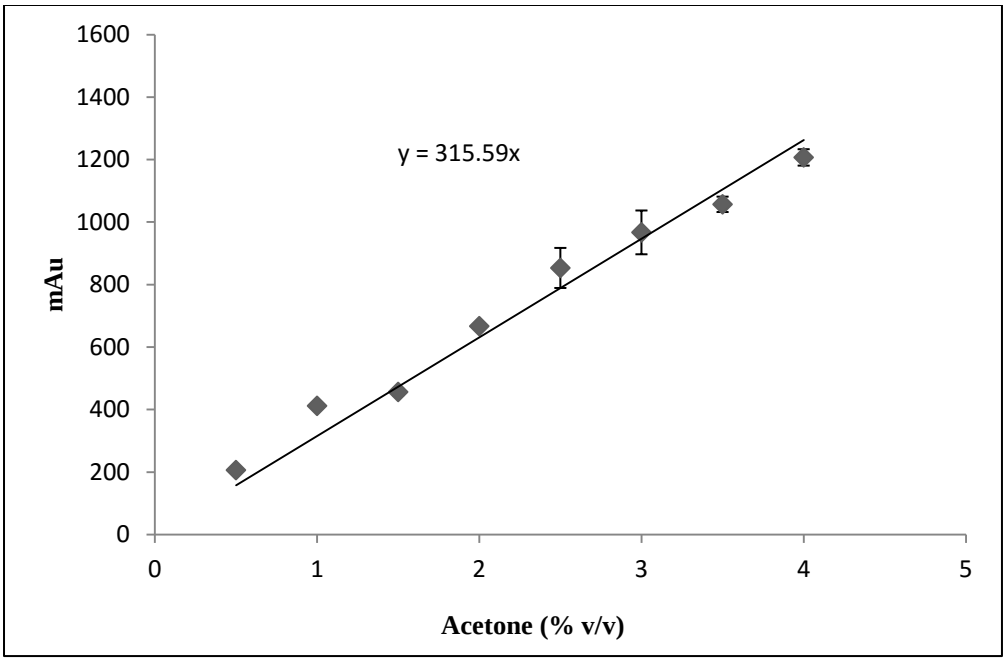

a)

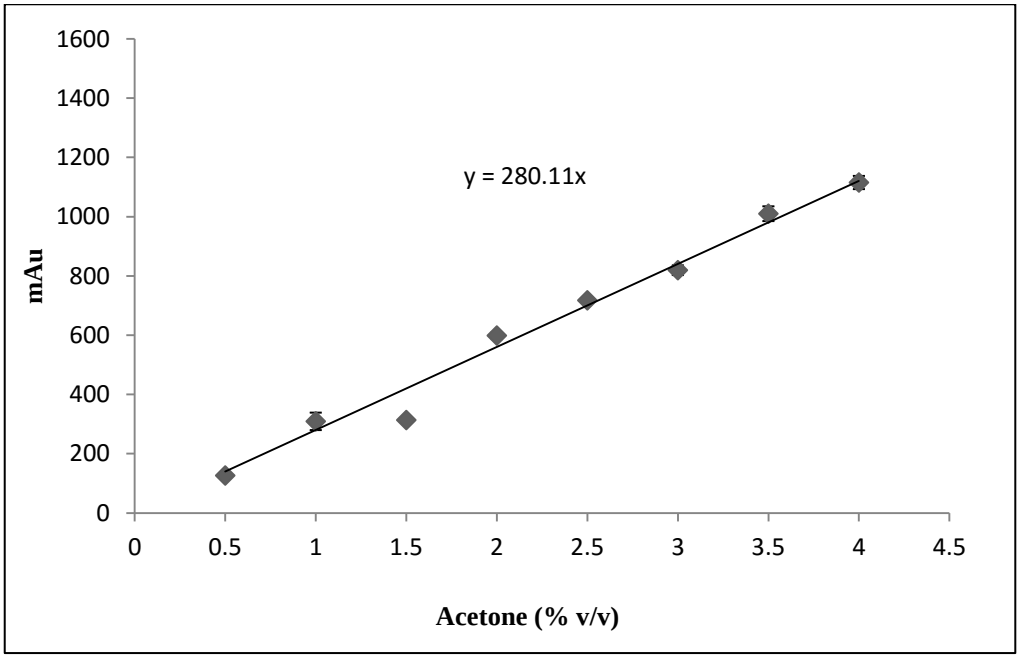

b)

Figure 31: Acetone calibration using pulse input method a) phosphate citrate buffer b) acetate buffer

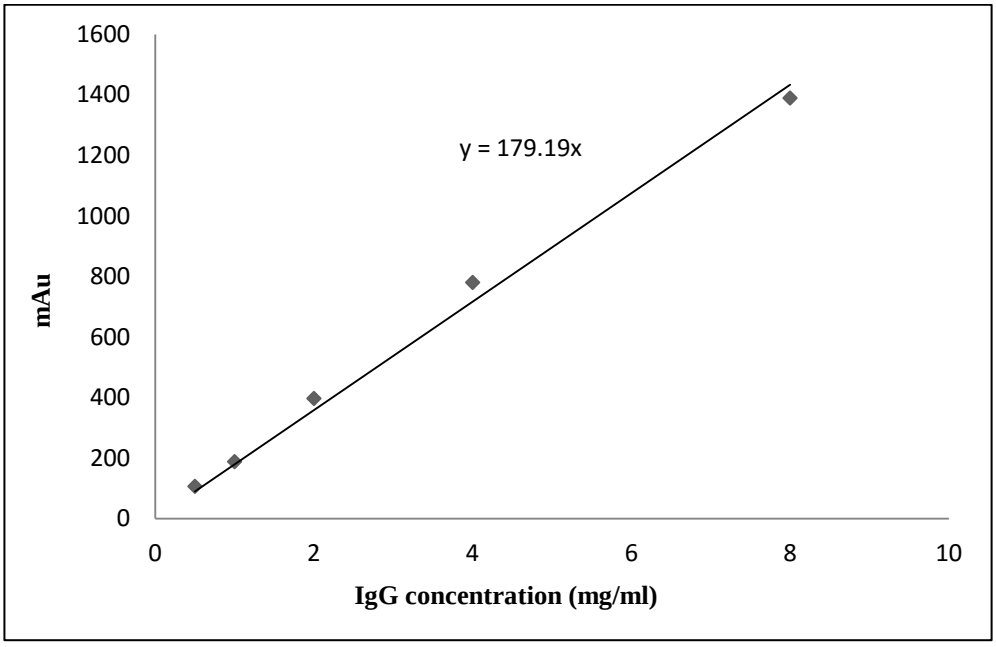

Figure 32: IgG Calibration with acetate buffer (pH 5)

Appendix B: t- test on overall system volume

Matlab Script file

```
clear all
clc

% t test Overall system volume (without membrane)

S1=[4.26 4.38 8.01 ];  % phosphate citrate buffer (ml)
S2= [7.49 4.06 4.99];  % acetate buffer (ml)

h1= ttest2(S1,S2)

% t test Overall system volume (Natrix C)

S11=[5.2 5.41 4.58];   % phosphate citrate buffer (ml)
S22= [5.83 6.55 5.73]; % acetate buffer (ml)


h2= ttest2(S11, S22)

% t test Overall system volume (Sartobind S)

x1=[4.16 4.47 5.1];  % phosphate citrate buffer (ml)
x2= [5.51 5.93 8.74]; % acetate buffer (ml)

h3= ttest2(x1, x2)




%Null hypothesis: The mean overall system volume for two different buffers
are equal
%h=1; rejection of null hypothesis at 5% significance level
%h=0; failure to reject null hypothesis at 5% significance level
```

Command window:

h1 = 0

h2 = 0

h3 = 0

Appendix C: Calculation for total porosity of membrane and interstitial velocity

Sample calculation for one run: Natrix C (With phosphate citrate buffer, Flow rate 10 ml/min)

- Outer diameter of the interior cylinder of the membrane holder, d= 0.029 m
- Thickness of the interior cylinder of the membrane holder, L= 0.005 m
- Flow rate during tracer experimentation, F'= 10 ml/min
- Flow rate during protein binding, F=1 ml/min

Mean Residence time/First moment of acetone, $\mu = \frac{\int_0^\infty t\, c(t)dt}{\int_0^\infty c(t)dt}$

Here c(t)= Tracer concentration measured at outlet of the system with time

The integrations in the mean residence time equation were estimated by using trapz(x,y) function in MATLAB (The matlab file is attached.)

μ= (0.028/0.1077) = 0.26 min

Total porosity of membrane, $\mathcal{E} = \frac{\mu F'}{\frac{\Pi d^2 L}{4}} = \frac{0.26\ \text{min} * 10\ \text{ml/min}}{\frac{3.1416 * 0.029^2\ \text{m}^2 * 0.005\ \text{m}}{4}} * \frac{1\text{m}^3}{10^6\ \text{ml}} = 0.79$

Interstitial velocity, $U = \frac{F}{\frac{\varepsilon \Pi d^2}{4}} = \frac{1\ \text{ml/min}}{\frac{0.79 * 3.1416 * 0.029^2\ \text{m}^2}{4}} * \frac{1\text{m}^3}{10^6\ \text{ml}} * \frac{1\ \text{min}}{60\text{s}} = 3.20\text{x}10^{-5}$ m/s

Matlab code for porosity and interstitial velocity calculation

```
clc
clear all
% Membrane porosity calculation using Pulse Experiment(run with Natrix
membrane_14 July)
%The first column of X is time in min, the second column is %Acetone
%(v/v)


X= [0.15    0.011359676
0.15    0.037029057
0.15    0.075293894
0.16    0.110824171
0.16    0.168243607
0.17    0.189660636
0.17    0.258918217
0.17    0.305440603
0.18    0.349887512
0.18    0.386850027
0.19    0.438277512
0.19    0.482724421
0.20    0.511480085
0.20    0.535470072
0.20    0.570433157
0.21    0.585943788
0.21    0.606213758
0.22    0.61722488
0.22    0.636651985
0.22    0.645299281
0.23    0.65879147
0.23    0.666355081
0.24    0.675075256
0.24    0.684156659
0.25    0.692889509
0.25    0.699882759
0.25    0.705389905
0.26    0.710592858
0.26    0.716042967
0.27    0.717079122
0.27    0.719873887
0.27    0.719880224
0.28    0.71758294
0.28    0.70908774
0.29    0.699331411
0.29    0.686726449
0.30    0.667651066
0.30    0.646208688
0.30    0.6106594
0.31    0.58441649
0.31    0.535184892
0.32    0.510456605
0.32    0.452143604
0.32    0.419804176
0.33    0.368674546
```

```
0.33    0.321169872
0.34    0.296913717
0.34    0.257352895
0.35    0.222519725
0.35    0.202024779
0.35    0.169707532
0.36    0.147837384
0.36    0.127985678
0.37    0.117098134
0.37    0.093146171
0.37    0.080943629
0.38    0.070262049
0.38    0.060977851
0.39    0.049519947
0.39    0.041462024
0.40    0.033743148
0.40    0.02436389
0.40    0.019205298
0.41    0.014683608
0.41    0.007750562
0.42    0.004810038];

t= X(:,1);
C= X(:,2); % %Acetone (v/v)

plot (t,C);
xlabel(' Time(min)')
ylabel ('% Acetone (v/v)')

% Mean Residence time calculation

K= C.*t;
N= trapz(t,K); %Numerator of mean residence time equation
D= trapz(t,C); %Denominator of mean residence time equation

Mean_residence_time=N/D % in minute

% Membrane Porosity Calculation

L=0.005; %Thickness of the interior cylinder of membrane holder (m)
d= 0.029; % Outer diameter of the interior cylinder of membrane holder (m)

V= ((pi*d^2*L)/4)*10^6 %Volume of the interior cylinder of the membrane
module in ml

F1= 10; %Flow rate in ml/min

Porosity= (Mean_residence_time*F1)/V %Total porosity of membrane

%Interstitial Velocity Calculation
F=1; % Flow rate during protein binding

U=((4*F)/(Porosity*pi*d^2))/(10^6*60)  %Interstitial Velocity in m/s
```

Appendix D: t-test on total porosity of membrane

Matlab Script file

```
clear all
clc

%Phosphate Citrate buffer
% t test for Natrix C porosity

S1=[ 0.788 0.811 0.874];  % membrane porosity values at 10 ml/min
S2= [0.894 0.779 0.688];  % membrane porosity values at 4 ml/min

h1= ttest2(S1, S2)

%Acetate buffer
% t test for Natrix C porosity

S11=[0.938 0.925 0.978];   % membrane porosity values at 10 ml/min
S22= [0.715 0.932 0.764];  % membrane porosity values at 4 ml/min


h11= ttest2(S11, S22)


%Phosphate Citrate buffer
% t test for Sartobind S porosity

x1=[0.737 0.853 0.795];  % membrane porosity values at 10 ml/min
x2= [0.795 0.768 0.8];   % membrane porosity values at 4 ml/min

h2= ttest2(x1, x2)

%Acetate buffer
% t test for Sartobind S porosity

x11=[0.978 0.936 0.911];   % membrane porosity values at 10 ml/min
x22= [0.855 0.666 0.795];  % membrane porosity values at 4 ml/min

h22= ttest2(x11, x22)


%Null hypothesis: The mean porosity value of a particular membrane at two
different flow
%rates for a particular buffer are equal.
%h=1; rejection of null hypothesis at 5% significance level
%h=0; failure to reject null hypothesis at 5% significance level
```

Command window:

h1 = 0

h11 = 0

h2 = 0

h22 = 1

Appendix E: Matlab code for dynamic modelling and calculation

Code for Sartobind S

```
function lsqmodelelangmuirsartobind
clear all
global C0 CIN D e kads kd L Np Ntime Q Q0 qmax tdeadpfr tf V Vdeadcstr
ymeasureint

% Sartobind S 0.5 g/l IgG, 100 min binding, 1st column is time (min), 2nd
% column is normalized concentration

ymeasure=measureddata;
tfmin=100;
Ntime=500;% number of time discretization
tmin = linspace(0,tfmin,Ntime);
ymeasureint=zeros(500,1);
%
% interpolation of the measured data
%
for i=1:Ntime
    ymeasureint(i)=interp1(ymeasure(:,1),ymeasure(:,2),tmin(i));
end

% Human IgG
MW=150000; %Molecular weight of IgG g/mol
C0= 0; % initial protein concentration (mol/m^3)
CIN=((0.5*1000)/MW); % inlet protein concentration (mol/m^3),0.5 g/L
D= 1.1e-10; %dispersion coefficient (m2/s), (Yang and Etzel, 2003)
kd=0.1; % in 1/s randomly selected
kads=1.9; % in m3.s/mol, (Yang and Etzel,2003)
qmax=((41*1000)/MW); % in mol/m3 (Hassel, 2015)
Q0=0;



% Membrane holder characteristics
Vdeadsys=6.73e-6; % Total dead volume of the system with Sartobind S and
acetate buffer(m^3)
Vdeadpfr=2.2e-6; % PFR Dead volume (m^3) (Yang and Etzel,2003)
Vdeadcstr=Vdeadsys-Vdeadpfr; % CSTR Dead Volume (m^3)
L=0.005;% Thickness of the interior cylinder of the membrane holder (m)
d=0.029; % Diameter of the interior cylinder of the membrane holder (m)
e=0.94; %Porosity
Q= 1/60/1000/1000; % Flow rate (m^3/s)
V=2.69e-5; %(m/s)


fprintf (' linear velocity : %e \n',V);
tau=L/V; % in second
fprintf (' process time : %e \n',tau);
tdeadpfr=Vdeadpfr/Q;
fprintf (' PFR delay time : %e \n',tdeadpfr);
```

```
tf=100*60;% final time (100 min for the experimental time, taken from Yan's
data)
Np=100; % number of space discretization
Ntime=500;% number of time discretization

lb=[0.1 0.01 0.01]; %lower bound of estimated parameter
ub=[20 40 1]; % upper bound of estimated parameter
%
% initial estimates
%
x0(1)=kads;
x0(2)=qmax;
x0(3)=kd;
%
% computation of the error of the model for this set of parameter
%
ferreur=erreur(x0);
SSE=ferreur'*ferreur;
display(SSE);
%
% lsqnonlin Non linear Least Square program
%
x = lsqnonlin(@erreur,x0,lb,ub);
%
% x contain the best estimate of the parameter
%
display(x);
ferreur=erreur(x);
SSE=ferreur'*ferreur;
display(SSE);
t = linspace(0,tf,Ntime);
%tdraw=t/tau;
Cout=modele(x);
%
% Breakthrough curve.
%
figure
plot(t,Cout,'k')
title('IgG binding with Sartobind S')
xlabel('Time (second)')
ylabel('C/Co')
hold on
plot (t,ymeasureint,'--')
legend (' Modelling curve (Solid line)','Experimental curve (Dotted line)')
%
% printing
%
fid = fopen('Resultatmatrix.txt', 'wt');
for i=1:Ntime
  fprintf(fid,' t = %14.10f %14.10f %14.10f
%14.10f\n',t(i),tmin(i),Cout(i),ymeasureint(i,1));
end
fclose (fid);
end
 %
```

```
 % computation of the prediction of the modele
 %
function f=modele(parameter)
global C0 CIN D e kads kd L Np Ntime Q Q0 qmax tdeadpfr tf V Vdeadcstr
ymeasureint
kads=parameter(1);
qmax=parameter(2);
kd=parameter(3);

f=zeros(Ntime,1);
x = linspace(0,L,Np);
t = linspace(0,tf,Ntime);

m = 0; % cartesian  (slab)
sol = pdepe(m,@pdex1pde,@pdex1ic,@pdex1bc,x,t); % Syntax for solving partial
differential equation
% Extract the first solution component as u.
u = sol(:,:,1)/CIN;
% CSTR model
f(1)=0;
Dt=tf/Ntime;
for i=1:Ntime-1
    CLc=u(i,end);
    f(i+1)=f(i)+Dt*Q/Vdeadcstr*(CLc-f(i));
end
end

function ecart=erreur(parameter)
global C0 CIN D e kads kd L Np Ntime Q Q0 qmax tdeadpfr tf V Vdeadcstr
ymeasureint
ecart=modele(parameter)-ymeasureint;
end
%
% PDE equation
%
function [coeft,f,s] = pdex1pde(x,t,u,DuDx)
global C0 CIN D e kads kd L Np Ntime Q Q0 qmax tdeadpfr tf V Vdeadcstr
ymeasureint
coeft = [1.0;1.0];
c=u(1);
q=u(2);
Ra=kads*c*(qmax-q)-kd*q;
DCDx=DuDx(1);
f = [D*DCDx;0];
s = [-V*DCDx-Ra*(1-e)/e;Ra];
end
% --------------------------------------------------------------
% Initial Condition
function u0 = pdex1ic(x)
global C0 CIN D e kads kd L Np Ntime Q Q0 qmax tdeadpfr tf V Vdeadcstr
ymeasureint
u0=[C0;Q0] ;
end
%
% --------------------------------------------------------------
```

```
% Boundary condition
% left is x=0: 0=D*dC/dx+V(CIN-C(0,t)
% right is x =Lc : D*dC/Dx=0
function [pleft,qleft,pright,qright] = pdex1bc(xl,ul,xr,ur,t)
global C0 CIN D e kads kd L Np Ntime Q Q0 qmax tdeadpfr tf V Vdeadcstr
ymeasureint
Cl=ul(1);
CINR=CIN*(t>tdeadpfr);
pleft = [V*(CINR-Cl);0];
qleft = [1;1];
pright = [0;0];
qright = [1;1];
end
function A=measureddata
A=[ 0.00    0
0.17    3.3484E-05
0.33    0.00017858
0.50    0.00011161
0.67    4.4645E-05
0.83    -0.00022323
1.00    -0.00051342
1.17    -0.00042413
1.33    -0.00036832
1.50    -0.000346
1.67    -0.00070316
1.83    -0.00051342
2.00    -0.00070316
2.17    -0.0008371
2.33    -0.00087058
2.50    -0.00080362
2.67    -0.00075897
2.83    -0.00095987
3.00    -0.0011831
3.17    -0.00123891
3.33    -0.001038
3.50    -0.00099336
3.67    -0.00093755
3.83    -0.00084826
4.00    -0.0009822
4.17    -0.00092639
4.33    -0.00102684
4.50    -0.00092639
4.67    -0.00091523
4.83    -0.00079245
5.00    -0.00052458
5.17    -0.00072549
5.33    -0.00043529
5.50    -0.00047994
5.67    -0.00026787
5.83    -0.00027903
6.00    -2.2323E-05
6.17    0.00043529
6.33    0.00047994
6.50    0.0011831
6.67    0.00225459
6.83    0.00364976
7.00    0.00619454
```

7.17	0.01120598
7.33	0.01514593
7.50	0.02347229
7.67	0.03428763
7.83	0.04929963
8.00	0.06889893
8.17	0.08730398
8.33	0.10858865
8.50	0.13631341
8.67	0.16776606
8.83	0.20176349
9.00	0.23912049
9.17	0.27911156
9.33	0.31687036
9.50	0.35556672
9.67	0.39937497
9.83	0.44266979
10.00	0.47272727
10.17	0.51828785
10.33	0.55739718
10.50	0.59570289
10.67	0.63246833
10.83	0.67103075
11.00	0.69103187
11.17	0.72729505
11.33	0.74724036
11.50	0.76288855
11.67	0.7948323
11.83	0.8180702
12.00	0.83627435
12.17	0.85768179
12.33	0.87173391
12.50	0.87920085
12.67	0.89582008
12.83	0.91181428
13.00	0.92091077
13.17	0.93657012
13.33	0.94689436
13.50	0.95358
13.67	0.96547798
13.83	0.97355879
14.00	0.98030024
14.17	0.99082538
14.33	1.0020202
14.50	1.00544673
14.67	1.01378425
14.83	1.01838272
15.00	1.01966628
15.17	1.02529159
15.33	1.04980189
15.50	1.03568279
15.67	1.0363748
15.83	1.05143144
16.00	1.04756962
16.17	1.05297171
16.33	1.06484737
16.50	1.06543892

16.67	1.07052849
16.83	1.07828562
17.00	1.07974775
17.17	1.08392209
17.33	1.09290697
17.50	1.09222613
17.67	1.09650092
17.83	1.10284056
18.00	1.10440315
18.17	1.10661309
18.33	1.1108544
18.50	1.11176963
18.67	1.11353312
18.83	1.11982812
19.00	1.11914727
19.17	1.12107819
19.33	1.1255204
19.50	1.1272504
19.67	1.12736202
19.83	1.13059881
20.00	1.13153636
20.17	1.13328869
20.33	1.13750767
20.50	1.13678219
20.67	1.13860148
20.83	1.14184943
21.00	1.14429377
21.17	1.14374686
21.33	1.14640326
21.50	1.14680507
21.67	1.14662649
21.83	1.15034321
22.00	1.14955076
22.17	1.14934985
22.33	1.1510687
22.50	1.15238574
22.67	1.15073386
22.83	1.15283219
23.00	1.15414923
23.17	1.1542162
23.33	1.15719627
23.50	1.15714047
23.67	1.15687259
23.83	1.15974106
24.00	1.15887047
24.17	1.15719627
24.33	1.16023216
24.50	1.16161616
24.67	1.15952899
24.83	1.16161616
25.00	1.16318991
25.17	1.16037725
25.33	1.16243094
25.50	1.16508734
25.67	1.16132597
25.83	1.16329036
26.00	1.16600257

26.17	1.16285507
26.33	1.16562308
26.50	1.16778838
26.67	1.16550031
26.83	1.16690664
27.00	1.17089123
27.17	1.16500921
27.33	1.16744238
27.50	1.17114794
27.67	1.16601373
27.83	1.16834645
28.00	1.17091356
28.17	1.16744238
28.33	1.16854735
28.50	1.1729784
28.67	1.16837993
28.83	1.16989787
29.00	1.17354763
29.17	1.16946258
29.33	1.17066801
29.50	1.17080194
29.67	1.16822367
29.83	1.16862548
30.00	1.1738155
30.17	1.16701825
30.33	1.17086891
30.50	1.17320163
30.67	1.16849155
30.83	1.17525532
31.00	1.17611474
31.17	1.17133769
31.33	1.1701211
31.50	1.17415034
31.67	1.1671187
31.83	1.1691389
32.00	1.17524415
32.17	1.16917239
32.33	1.17100285
32.50	1.17413918
32.67	1.17064568
32.83	1.17093588
33.00	1.17279982
33.17	1.16721915
33.33	1.17109214
33.50	1.17437357
33.67	1.17139349
33.83	1.17210782
34.00	1.17341369
34.17	1.16793348
34.33	1.16075674
34.50	1.15148167
34.67	1.14033149
34.83	1.14865785
35.00	1.16701825
35.17	1.17158324
35.33	1.17911714
35.50	1.18401697

35.67	1.1848429
35.83	1.18878286
36.00	1.19198616
36.17	1.19098164
36.33	1.19439701
36.50	1.19726547
36.67	1.19334784
36.83	1.19478766
37.00	1.19617166
37.17	1.19604889
37.33	1.19648418
37.50	1.19671857
37.67	1.19707573
37.83	1.19828115
38.00	1.19848206
38.17	1.19724315
38.33	1.19751102
38.50	1.19838161
38.67	1.1984709
38.83	1.19911825
39.00	1.19991071
39.17	1.19897316
39.33	1.19883922
39.50	1.20108265
39.67	1.2001451
39.83	1.2002009
40.00	1.2021653
40.17	1.20119426
40.33	1.20156259
40.50	1.20263408
40.67	1.20154026
40.83	1.20035716
41.00	1.20287962
41.17	1.20150678
41.33	1.20136168
41.50	1.20327027
41.67	1.2034935
41.83	1.20213182
42.00	1.20366092
42.17	1.20330376
42.33	1.20258943
42.50	1.20429711
42.67	1.20358279
42.83	1.20315866
43.00	1.2045315
43.17	1.20462079
43.33	1.20274569
43.50	1.20492215
43.67	1.20484402
43.83	1.20322563
44.00	1.20566996
44.17	1.20514538
44.33	1.20441989
44.50	1.20709861
44.67	1.20617222
44.83	1.20508957
45.00	1.20705397

45.17	1.20712093
45.33	1.20527931
45.50	1.20761203
45.67	1.20725487
45.83	1.20639545
46.00	1.20839333
46.17	1.20854958
46.33	1.20707629
46.50	1.20847145
46.67	1.20905184
46.83	1.20898488
47.00	1.21049166
47.17	1.21078185
47.33	1.21044701
47.50	1.21120598
47.67	1.21190915
47.83	1.21110553
48.00	1.21212121
48.17	1.21257883
48.33	1.21196495
48.50	1.2125007
48.67	1.21283554
48.83	1.21193147
49.00	1.21266812
49.17	1.21338244
49.33	1.21202076
49.50	1.21341593
49.67	1.21399632
49.83	1.21276857
50.00	1.21430883
50.17	1.21473297
50.33	1.21392935
50.50	1.21468832
50.67	1.21553658
50.83	1.21491155
51.00	1.21586026
51.17	1.21609465
51.33	1.21531335
51.50	1.21608349
51.67	1.21621742
51.83	1.21543613
52.00	1.21579329
52.17	1.21659691
52.33	1.21546961
52.50	1.21620626
52.67	1.21644065
52.83	1.21557007
53.00	1.21572632
53.17	1.21702104
53.33	1.21591607
53.50	1.21568168
53.67	1.2168871
53.83	1.21645181
54.00	1.21543613
54.17	1.21706568
54.33	1.21651878
54.50	1.21574865

54.67	1.21721078
54.83	1.21702104
55.00	1.21533568
55.17	1.21714381
55.33	1.21824879
55.50	1.21686478
55.67	1.2185055
55.83	1.21860595
56.00	1.2171773
56.17	1.21859479
56.33	1.21911937
56.50	1.21738936
56.67	1.2187064
56.83	1.22001228
57.00	1.21837156
57.17	1.21916402
57.33	1.22042525
57.50	1.2187064
57.67	1.21944305
57.83	1.22034712
58.00	1.21844969
58.17	1.21911937
58.33	1.22034712
58.50	1.21813717
58.67	1.21937608
58.83	1.22049221
59.00	1.21853898
59.17	1.21945421
59.33	1.22031363
59.50	1.21942073
59.67	1.22016854
59.83	1.22057034
60.00	1.21910821
60.17	1.21985602
60.33	1.22001228
60.50	1.21952118
60.67	1.2202355
60.83	1.22069312
61.00	1.2196886
61.17	1.22086054
61.33	1.22163067
61.50	1.2240192
61.67	1.22159719
61.83	1.22196551
62.00	1.22031363
62.17	1.22100564
62.33	1.2219097
62.50	1.22161951
62.67	1.22179809
62.83	1.22263519
63.00	1.2218539
63.17	1.22209945
63.33	1.22315977
63.50	1.22333836
63.67	1.22304816
63.83	1.22342765
64.00	1.223383

64.17	1.22368436
64.33	1.2245103
64.50	1.22356158
64.67	1.22245661
64.83	1.22447681
65.00	1.22371784
65.17	1.22317094
65.33	1.22492327
65.50	1.22494559
65.67	1.22463307
65.83	1.22555946
66.00	1.22541436
66.17	1.22380713
66.33	1.22536972
66.50	1.22519114
66.67	1.22533624
66.83	1.22616217
67.00	1.22663095
67.17	1.22654166
67.33	1.22721134
67.50	1.22907528
67.67	1.22563759
67.83	1.22850606
68.00	1.22717786
68.17	1.22535856
68.33	1.2270216
68.50	1.22769128
68.67	1.22596127
68.83	1.22725599
69.00	1.22793683
69.17	1.22670908
69.33	1.22776941
69.50	1.22826051
69.67	1.22670908
69.83	1.22823818
70.00	1.22831631
70.17	1.22742341
70.33	1.22907528
70.50	1.22942128
70.67	1.22680953
70.83	1.22945477
71.00	1.23015793
71.17	1.22798147
71.33	1.23025838
71.50	1.2312071
71.67	1.22908644
71.83	1.23074948
72.00	1.23163123
72.17	1.2298789
72.33	1.2318991
72.50	1.23265807
72.67	1.23041464
72.83	1.231754
73.00	1.23291478
73.17	1.23122942
73.33	1.23188794
73.50	1.23327195

73.67	1.23165355
73.83	1.23217813
74.00	1.23299291
74.17	1.23103968
74.33	1.2321893
74.50	1.2335175
74.67	1.23134103
74.83	1.23139684
75.00	1.23403092
75.17	1.23160891
75.33	1.23198839
75.50	1.23410905
75.67	1.23144149
75.83	1.2316982
76.00	1.23404208
76.17	1.23198839
76.33	1.2321893
76.50	1.23360679
76.67	1.23195491
76.83	1.23187678
77.00	1.23338356
77.17	1.23250181
77.33	1.23217813
77.50	1.23448853
77.67	1.23310453
77.83	1.23207768
78.00	1.23464479
78.17	1.23416485
78.33	1.23269156
78.50	1.23578325
78.67	1.23564931
78.83	1.23341704
79.00	1.23627435
79.17	1.23638596
79.33	1.23407556
79.50	1.23631899
79.67	1.23669848
79.83	1.23416485
80.00	1.23718958
80.17	1.23654222
80.33	1.23453318
80.50	1.23807132
80.67	1.23636364
80.83	1.23531447
81.00	1.23924326
81.17	1.23778113
81.33	1.23682125
81.50	1.23891958
81.67	1.23946649
81.83	1.23838384
82.00	1.24029243
82.17	1.24018081
82.33	1.23913165
82.50	1.24061611
82.67	1.24009152
82.83	1.238395
83.00	1.24037056

83.17	1.23916513
83.33	1.23736816
83.50	1.23798203
83.67	1.23875216
83.83	1.23814945
84.00	1.23835035
84.17	1.23889726
84.33	1.23797087
84.50	1.23968971
84.67	1.2409063
84.83	1.23975668
85.00	1.23935487
85.17	1.24008036
85.33	1.24050449
85.50	1.24042636
85.67	1.24086166
85.83	1.24044869
86.00	1.23913165
86.17	1.23973436
86.33	1.24031475
86.50	1.23919862
86.67	1.24063843
86.83	1.24077236
87.00	1.2393772
87.17	1.2411965
87.33	1.2419443
87.50	1.2402143
87.67	1.24143088
87.83	1.24127462
88.00	1.23929907
88.17	1.2410514
88.33	1.24236844
88.50	1.23997991
88.67	1.24095095
88.83	1.24156482
89.00	1.23952229
89.17	1.2413974
89.33	1.24207824
89.50	1.24050449
89.67	1.24112953
89.83	1.24205592
90.00	1.24042636
90.17	1.24163179
90.33	1.24281489
90.50	1.2411965
90.67	1.24293766
90.83	1.2430716
91.00	1.24152017
91.17	1.24201127
91.33	1.2420894
91.50	1.24116301
91.67	1.24233495
91.83	1.24348457
92.00	1.24091746
92.17	1.2420894
92.33	1.24230147
92.50	1.24124114

```
92.67   1.24186618
92.83   1.2422345
93.00   1.24138624
93.17   1.2412523
93.33   1.24269211
93.50   1.24173224
93.67   1.24146437
93.83   1.2415425
94.00   1.24062727
94.17   1.24028127
94.33   1.24230147
94.50   1.24182153
94.67   1.24118533
94.83   1.24193314
95.00   1.2420894
95.17   1.24170992
95.33   1.24200011
95.50   1.24270328
95.67   1.24285953
95.83   1.24400915
96.00   1.24301579
96.17   1.24349573
96.33   1.24432167
96.50   1.24320554
96.67   1.24252469
96.83   1.24442212
97.00   1.24493554
97.17   1.24251353
97.33   1.24490206
97.50   1.24539316
97.67   1.24423238
97.83   1.24468999
98.00   1.24617445
98.17   1.24436632
98.33   1.24531503
98.50   1.24616329
98.67   1.24367431
98.83   1.24531503
99.00   1.24644232
99.17   1.24510296
99.33   1.24571684
99.50   1.24608516
99.67   1.24479045
99.83   1.24505832
100.00  1.24611865];
    end
```

Command window:

x =

5.8861 0.9140 0.7663

SSE =

20.4721

Unit conversion of the estimated Langmuir parameters

$k_a = 5.89 \frac{m^3}{mol.s} * \frac{10^6 ml}{1m^3} * \frac{mol}{150000\ g} * \frac{1g}{10^3\ mg} = 3.92 \times 10^{-2}$ ml/mg.s

$q_{max} = 0.91 \frac{mol}{m^3} * \frac{1m^3}{10^6\ ml} * \frac{150000g}{mol} * \frac{10^3\ mg}{1g} = 136.5$ mg/ml

$k_d = 0.77\ s^{-1} = 77 \times 10^{-2}\ s^{-1}$